Open Access

Advances in Environmental and Engineering Research

LIDSEN Publishing Inc.

Original Research

Sustainable Water Management Using Rainfall-Runoff Modelling in Rift Valley Basin, East Africa

Agegnehu Kitanbo Yoshe *

Department of Water Resources and Irrigation Engineering, Arba Minch University, 21 Post Office Box, Arba Minch, Ethiopia; E-Mail: kitanbo@gmail.com

* **Correspondence:** Agegnehu Kitanbo Yoshe; E-Mail: kitanbo@gmail.com

Academic Editor: Wen-Cheng Liu

Special Issue: Advances in Hydrology, Water Quality and Sediment Simulation Modelling

Adv Environ Eng Res
2025, volume 6, issue 1
doi:10.21926/aeer.2501003

Received: September 03, 2024
Accepted: December 19, 2024
Published: January 06, 2025

Abstract

Managing water resources offers crucial information about the availability of water supplied from catchments into water bodies, which plays a vital role in water resource engineering. However, due to changes in the global climate, hydrological modeling of river catchments is critically crucial for socio-economic development and livelihoods. Numerous models evaluate runoff from precipitation, but the SCS-CN method is fundamental and the most widely recognized for calculating runoff. This research evaluates runoff depth in the Rift Valley River basin using the SCS-CN model and remote sensing techniques from 1991 to 2022 based on precipitation data availability. The 37861 km² (65.75%) of the study area was covered by the hydrological soil group "C," and 19729 km² (34.26%) was by the hydrological soil group "D." The land use classification shows that approximately 2556.65 km² (4.44%) is water, 9003.72 km² (15.63%) is tree cover, 144.3 km² (0.25%) is flooded vegetation, 19012.21 km² (33.01%) is cropland, 3122.07 km² (5.42%) is built-up area, 984.29 km² (1.71%) is bare land, and 22763.82 km² (39.53%) is rangeland, which covers the largest area in the study region. The evaluated curve numbers for the study area were 74.71 for normal soil moisture conditions (AMC-II), 55.37 for dry soil moisture conditions (AMC-I), and 87.20 for wet soil moisture conditions (AMC-III). The evaluated probable maximum retention capacity (S) was 213.73 for AMC-I,

94.98 for AMC-II, and 46.38 for AMC-III. The preliminary abstraction loss (Ia) was 42.75 for AMC-I, 19.00 for AMC-II, and 9.280 for AMC-III. The higher the value of maximum retention (S) and Ia, the more maximum retention and maximum abstraction loss, which leads to low runoff depth, whereas the smallest value of S and Ia represents less retention and less abstraction loss, demonstrating high runoff depth. As a result, the average annual surface runoff calculated for the Rift Valley River Basin from 1991 to 2022 was observed to be 787.425 mm per year, with a total volume of approximately 45347805750 m^3/year. The maximum rainfall recorded was 1047.11 mm in 2020, while the minimum was 673.22 mm in 2021. From the evaluated results, the estimated average rainfall runoff varies between 562.70 and 1047.1 mm, and the average volume of rainfall-runoff ranges from 32403589400 to 60303064900 Cubic Meters. The spatial distribution of runoff shows a significant variation in the study period between 2011 and 2022, which was essential to identify hotspot areas for water resource management. This data is valuable for watershed development, effective planning of water resources, sustainable ecological practices, and groundwater recharge initiatives. Moreover, the SCS-CN and GIS techniques have proven effective, requiring less time and resources to manage large datasets across broader environmental regions for identifying potential sites for artificial recharge structures.

Keywords
Water resource management; rainfall-runoff modeling; spatiotemporal variation of runoff; SCS-CN model and GIS techniques

1. Introduction

Examining water resources and river basin problems stands at the forefront of environmental research, presenting a critical nexus between human societies and the intricate ecosystems they inhabit [1, 2]. Sustainable water resource management has become increasingly urgent against the global challenges posed by climate change and population growth. Rivers, the lifeblood of countless civilizations, play an irreplaceable role in facilitating agriculture, industry, energy production, and freshwater supply [3]. Consequently, comprehension and mitigation of river basin issues are paramount for preserving biodiversity, protecting human livelihoods, and equitable access to these invaluable resources. The consequences of the unmitigated river basin issue can be far-reaching, with potential effects that extend both regionally and globally. Unpredictable surface runoff in river basins, stemming from changing precipitation patterns, deforestation, and transformations in land use, can lead to catastrophic floods or devastating droughts [4]. Communities residing along river areas face an increased risk of displacement, infrastructure damage, and economic losses, thereby exacerbating issues of social inequality [5, 6]. In light of these considerations, administrative and research-oriented steps are essential to implement sustainable water resource management strategies. Such steps should delve into the complexity of river surface runoff, promote resilience, and foster harmony between human activities and the natural environment [7-9].

Hydrologists have faced a fundamental challenge in flood forecasting in ungauged and/or poorly gauged basins for decades. Simulating reliable continuous streamflow has been an essential and

common objective for the scientific hydrological community since the middle of the 20th century. Such an issue is paramount for addressing engineering and environmental problems, which span from designing hydraulic structures to flood-risk assessment and stormwater management, from forecasting the climatic, groundwater Replenishment and anthropogenic effects on water resources to assessing economic benefits from hydropower production. Additionally, rainfall-runoff models are the most common tools for predicting discharge and estimating water balance. The study of rainfall-runoff estimation is a critical problem in hydrological modeling. Because of this context, it is recommended that accurate hydrological prediction is essential for water resource planning and management, mentoring lakes and dams to avoid soil erosion and to replace groundwater [10, 11]. The problem that arises most frequently in hydrological research is the importance of estimating runoff from a river basin where there are precipitation records but no runoff records [12]. Hence, runoff is one of the most important hydrological variables used in most applications involving water resources [13]. Collecting this data is costly, time-consuming, and challenging [14], hence the advantage of hydrological models for estimating runoff from a river basin. So, the hydrological models are grouped into physical process-based models, empirical-based models, data-driven models, and conceptual models used for runoff estimation [15-17]. Conceptual hydrological models, sometimes called gray-box models, are precipitation-runoff models built based on observed or assumed empirical relationships among different hydrological variables. They differ from black-box models, which only statistically consider the precipitation-runoff relationship. They also differ from the physically distributed hydrological models based on solving differential equations describing the physical laws of mass, energy, and momentum conservation. Data-driven hydrological models are widely used for many practical purposes. However, the reliability of such models depends heavily on the strategy used to partition available observations into model calibration and evaluation subsets. An empirical model is built upon the observation of input and output without seeking to represent explicitly the process of conversion. In physically based hydrologic modeling, the hydrologic process of water movement is modeled either by the finite difference approximation of the partial differential equation representing the mass, momentum, and energy balance or by empirical equations. For example, the SCS-CN model, the Horton model, and the Green Ampt infiltration model, etc., are empirical methods [18]; the Sacramento model, the Stanford model, etc., are conceptual models [19]; SHE models, SWAT models, etc., are physical process-based models [20]; and data-driven models are machine learning and deep learning [21]. The Soil Conservation Service Curve Number (SCS-CN) method (SCS, 1993) is commonly used to estimate the depth of surface runoff in a watershed for a given rainfall event. The Natural Resource Conservation Service Curve Number (NRCS-CN) method has recently been renamed. The process is simple and valuable for ungauged watersheds and accounts for four major runoff-producing watershed characteristics: soil type, land use/treatment, surface condition, and antecedent moisture conditions. The method has been a topic of much discussion in hydrologic literature for the last three decades.

In the late 1940s, Sherman [22] proposed building a relationship between rainfall and runoff via unit hydrograph theory. Later, Mockus [23] suggested the inclusion of variables like land use, land cover type, soil, antecedent moisture condition, spatial distribution, etc. To evaluate the surface runoff based on infiltration rate, Musgrave [24] classified soil into four classes, namely A, B, C, and D. This classification was based on SCS-CN methods [25] that provide an empirical relationship to estimate runoff that considers initial abstraction based on land use, land cover, and soil type, called the SCS-CN method. The SCS-CN method is the most popular model due to its simplicity [26, 27].

SWAT and HEC-HMS also use the SCS-CN model to calculate surface runoff [28, 29]. Initially, the SCS-CN model was developed for small watersheds in the USA to estimate direct surface runoff from small rainfall events; then, it was used for several areas, climate conditions, and land uses [30, 31]. Due to increasing urbanization, land use and land cover patterns drastically changed, which influenced SCS-CN and hydrological parameters affecting runoff from the catchments [32].

Advancements in geospatial technologies help include these variables for evaluating runoff from watersheds spatially and temporally. Different remote sensing products from satellites like IRS, NOAA, Landsat, TRMM, etc. can obtain reliable input parameters like precipitation, soil type, land use type, DEM, etc., from a regional to global scale [33]. In the present study, the SCS-CN model, which belongs to empirical models, was used due to its reliability and popularity among the hydrological models [34-36] with GIS; hence, the majority of researchers used GIS in conjunction with the curve numbers approach, which has been proven to be quick and accurate for estimating runoff [16]. This modeling of runoff and identifying the best locations for collecting water or recharging underground water using GIS and remote sensing have shown that this is an essential tool [37]. RS and GIS data are more dependable, modern, and quick than traditional techniques, and they are vital for gathering data on many elements of land use and soil type to create curve numbers, which are particularly important for runoff estimation [38]. Hence, hydrological research can be conducted accurately using GIS and RS technology, and GIS and RS data are becoming more prevalent in planning the development and management of natural resources. In particular, GIS supports decision-making by integrating multiple datasets and performing spatial analysis [39]. The curve number runoff model is helpful in predicting the direct runoff volume for any specific rainfall events using antecedent moisture conditions [40] and also for different tools and software developed to capture and process remote sensing and GIS data for runoff modeling. But either they are expensive or require large computer hardware [41]. Few free and open-source platforms are available for water resource studies [42] but require advanced skills. Presently, no model can include the temporal changes or dynamics of LULC changes in the process, and changes can only be accommodated by repeating the entire simulation process. This problem becomes more severe if the data to be analyzed is spatially and temporally larger or has multiple parameters. Spatial data have made it possible to accurately predict the runoff, which has led to significant increases in its use in hydrological applications. The curve number method [43] is adaptable and widely used for runoff estimation. This method is an essential property of the watershed, specifically soil permeability, land use, and antecedent soil water conditions, which are considered [44]. The SCS-CN approach is also commonly employed in studies measuring the influence of wildfires on the hydrological response of vegetated regions and consequent hydrological risks [45, 46].

A chain of lakes and wetlands with unique hydrological and ecological characteristics characterizes the Rift Valley Basin. Largely foreign and national horticulture and floriculture enterprises have been settling in the area recently. Still, the crisis of water for drinking and irrigation purposes has adversely affected human society and has also been affected by drought events. Drought is a natural disaster in every climatic condition, adversely affecting socio-economic and environmental degradation [47]. In the study area, agriculture is utilized chiefly. It depends on rainfall systems, but rainfall deficiency is one of the significant fundamental causes of drought occurrences, and it is considered the meteorological drought, which is also responsible for the occurrences of hydrological, agricultural, and socio-economic drought. First, factors like topographical, climatic, and geological conditions are responsible for frequent drought occurrences

and associated water scarcity in the study area. To overcome the water shortage problem in this water-scarce area, it is important to analyze rainfall-runoff, as it estimates the discharge rate of the river basin, to conserve water resources and ensure sustainable watershed management in the study area. No such investigation has been noted in the existing literature on the area studied. As a result, the techniques used, the methodology for estimating rainfall runoff, and the final result will be regarded as a new and honest contribution to the present study area. In general, this study aims to estimate rainfall runoff using the SCS-CN model in the Rift Valley basin through GIS and remote sensing. Therefore, the methodology applied in this study is quite helpful in characterizing rainfall runoff and associated water shortage problems, which is the novelty of this study. The present study would fill the research gap in rainfall-runoff dynamics in the data-scarred Rift Valley basin. Moreover, the present study will also fulfill the needs of different stakeholders for sustainable watershed management and water resource planning.

2. Method and Materials

2.1 Description Study Area

The study was located in the southern Ethiopian Rift Valley basin, located between 36°–40° E and 4°–9° N. A complex and rugged topography characterizes the basin. Based on the digital elevation model data, the elevation of the area ranges from 450 to 4190 m above sea level, and western and eastern escarpments bound it with altitudes of up to 4190 m above sea level. The basin contains lakes, forests, grasslands, wetlands, and savannahs, which provide a range of ecosystem services, e.g., as a natural habitat for diverse birds, fish, and wildlife species. It contains over 500 bird species of African, European, Arabian, and Asian origin and 33 fish species [48]. In particular, many lakes in the region are a focal point for internationally significant numbers of wildfowl and water and rated or endangered species. Additionally, BirdLife International has identified it as one of the most important bird habitats in the world [49]. Figure 1 shows the location map of the study area.

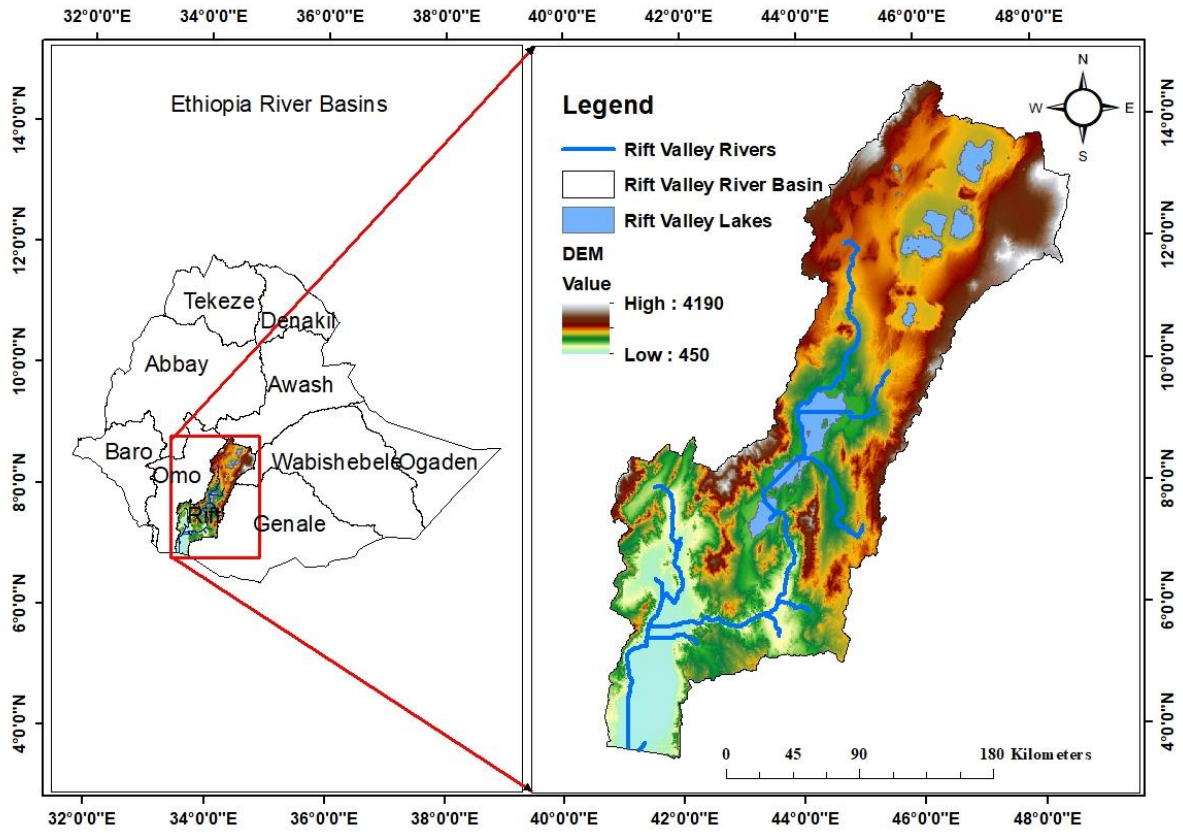

Figure 1 Location map of Rift Valley Basin in Ethiopia.

2.2 Methods and Data Collection

The methodology used to analyze the characteristics of rainfall-runoff for the study area using the GIS-based SCS-CN method is presented in Figure 2. To estimate rainfall runoff, different types of secondary data were used to generate various thematic layers, such as land use, slope, DEM, and soil textural map. The secondary data was collected from multiple sources. The main inputs required for the SCS-CN are as follows: watershed boundary and slope map from the digital elevation model from USGS datasets; the land use land cover map obtained from MCD12Q1.006 MODIS Land cover [50]; the hydrological soil group generated from the World Food and Agriculture Organization (HYSOGS250m) [51]; and rainfall data collected from Climate Hazards Group InfraRed Precipitation (CHIRPS) with station data [52]. In this model, land use is categorized by antecedent moisture conditions, which are integrated with GIS to estimate the curve number value of the hydrological soil group [53]. Then the rainfall-runoff for the watershed can be calculated using the computed weighted curve number incorporated into a GIS system for quick and precise assessment of runoff curve numbers [54, 55].

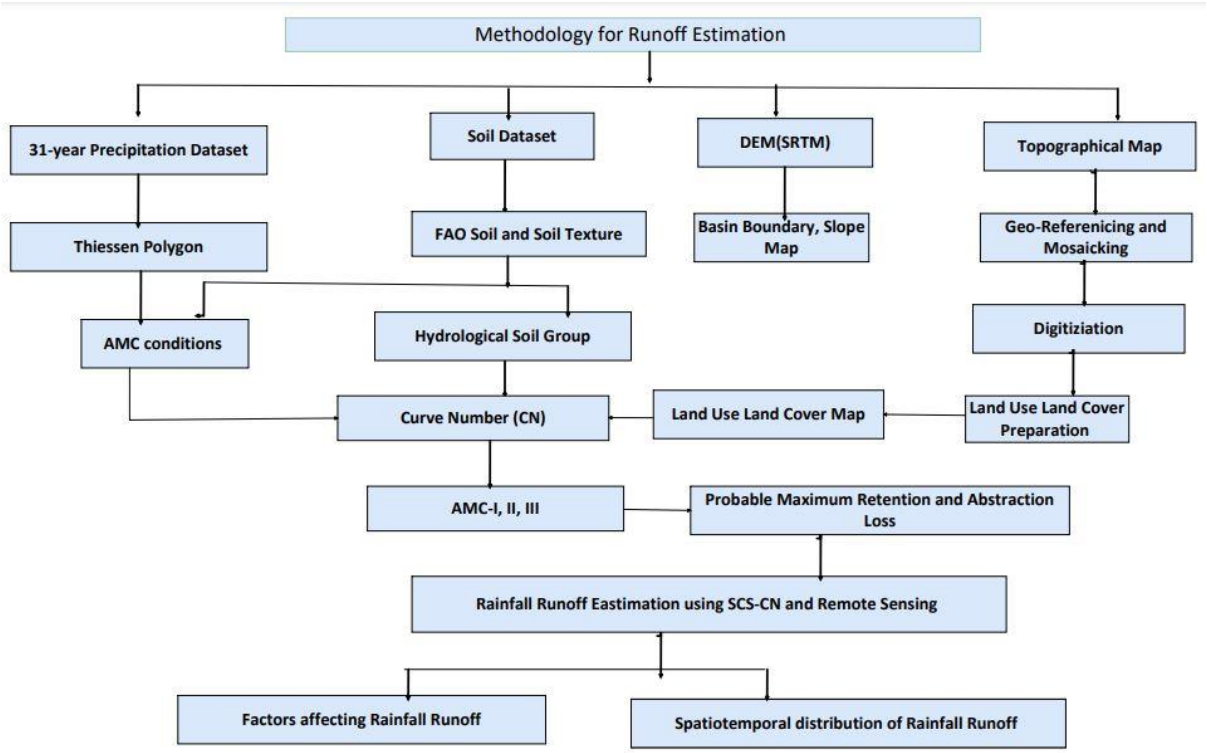

Figure 2 Methodology for estimation of rainfall runoff in Rift Valley basin.

2.2.1 Precipitation

The most important source of fresh water on Earth is precipitation, a crucial part of the water cycle. Approximately 505,000 cubic kilometers of water falls as precipitation yearly, 398,000 cubic kilometers over the oceans and 107,000 cubic kilometers over land. So, the SCS-CN method uses the precipitation data as input to estimate river basin runoff and discharge [55]. But surface runoff creation is affected by precipitation. Therefore, when precipitation is excessive, there is a corresponding increase in surface runoff. However, the characteristics of the land surface, such as land use and soil textural conditions, can affect surface runoff either directly or indirectly [56]. Fuka et al. [57] highlighted that the weather value generated by CFSR for river basin simulations is as good as or better than the weather value used in simulations generated by conventional meteorological stations. For this study, area precipitation data was extracted from climate forecast system reanalysis (CFSR) [58]. The spatial distribution of the precipitation for the study area ranges from 33.812 to 141.79 and is presented in Figure 3.

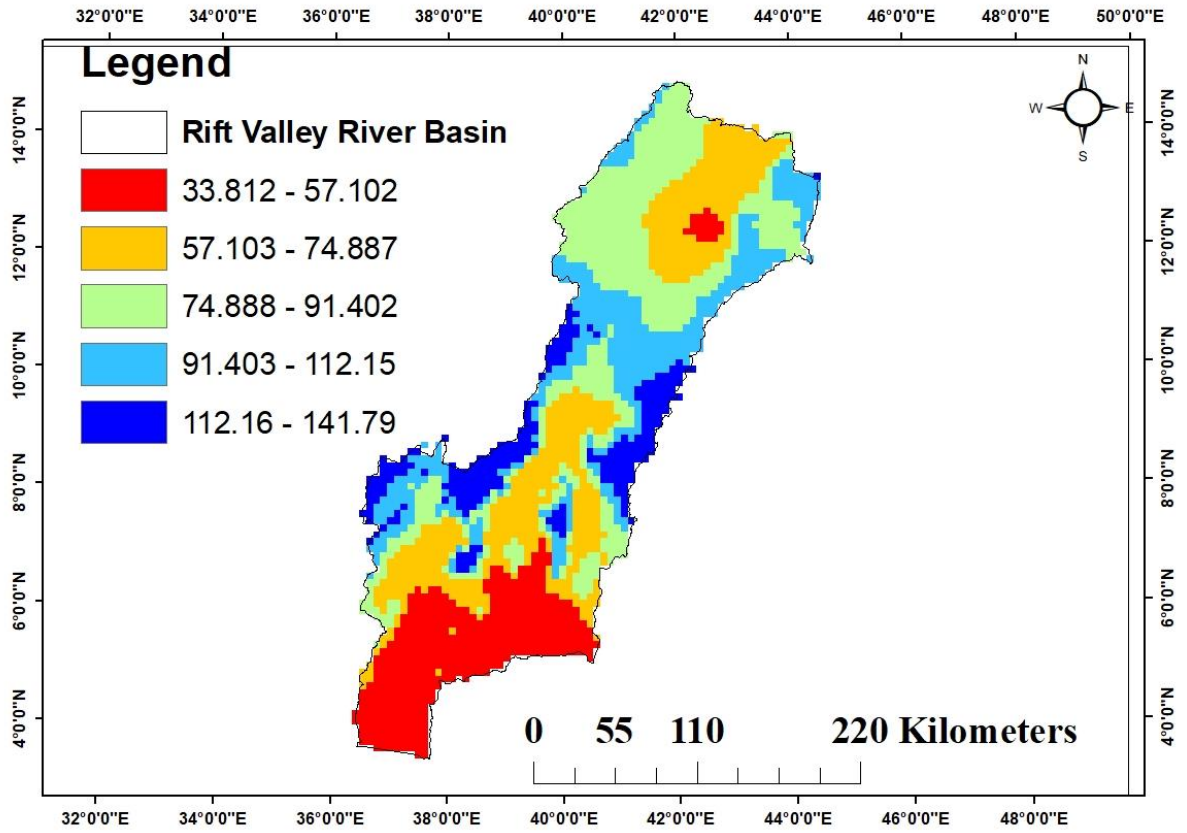

Figure 3 Characteristics of precipitation in Rift Valley basin.

2.2.2 Digital Elevation Model (DEM)

The SCS-CN model requires DEM as a primary and necessary input variable to calculate flow accumulation, stream networking, catchment boundary, slope, and others [59]. Moreover, watershed delineation is the area that includes all the land and the contributors of runoff water to the central location. But every watershed has unique features, such as gradient, form, area size, drainage, vegetation cover, soil type, landforms, land use, and climatic conditions. Therefore, watershed management indicates the wise utilization of all the land and water resources in the river basin for optimal output with the least risk to the natural resources. Due to that, the DEM is an elevation model that restores the dataset in pixel or grid format. The spatial resolution used for this study is an arc-second 30m global digital elevation model from USGS (https://earthexplorer.usgs.go), used in GIS and presented in Figure 4.

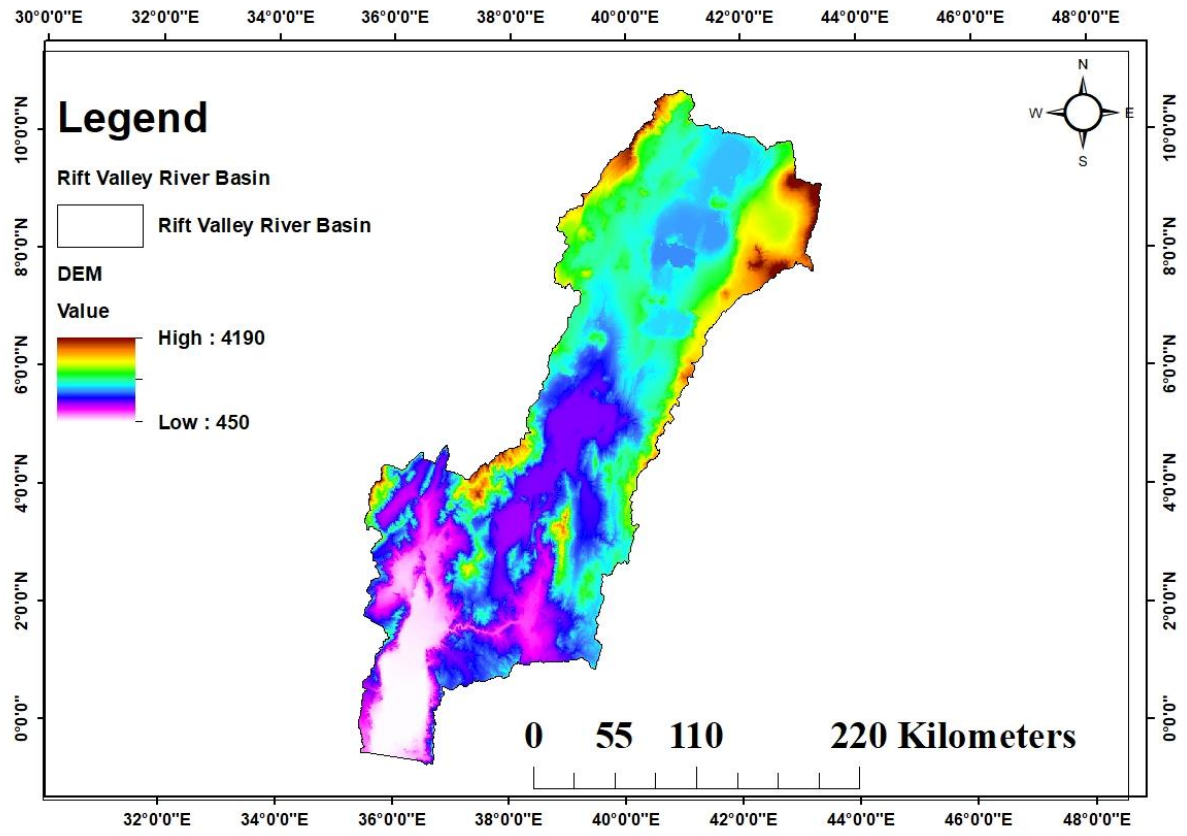

Figure 4 Characteristics of Digital elevation model in Rift Valley basin.

2.2.3 Slope

The slope is an essential topographical feature, explained by the contour area and horizontal spacing. It is crucial to determine surface runoff, infiltration, and groundwater recharge [60-63]. The slopes in the study area are extracted from the DEM using spatial analysis tools in the GIS environment. The hill has a vital role in calculating rainfall runoff and estimating groundwater recharges [64]. Reclassification of the slope depends on its steepness and flatness. When the slope is flat, the rainfall-runoff over the land surface is slow, which increases infiltration, whereas when the slope is steep, the rainfall-runoff is high with a low infiltration rate. The area's slope was classified into five classes and presented in Figure 5.

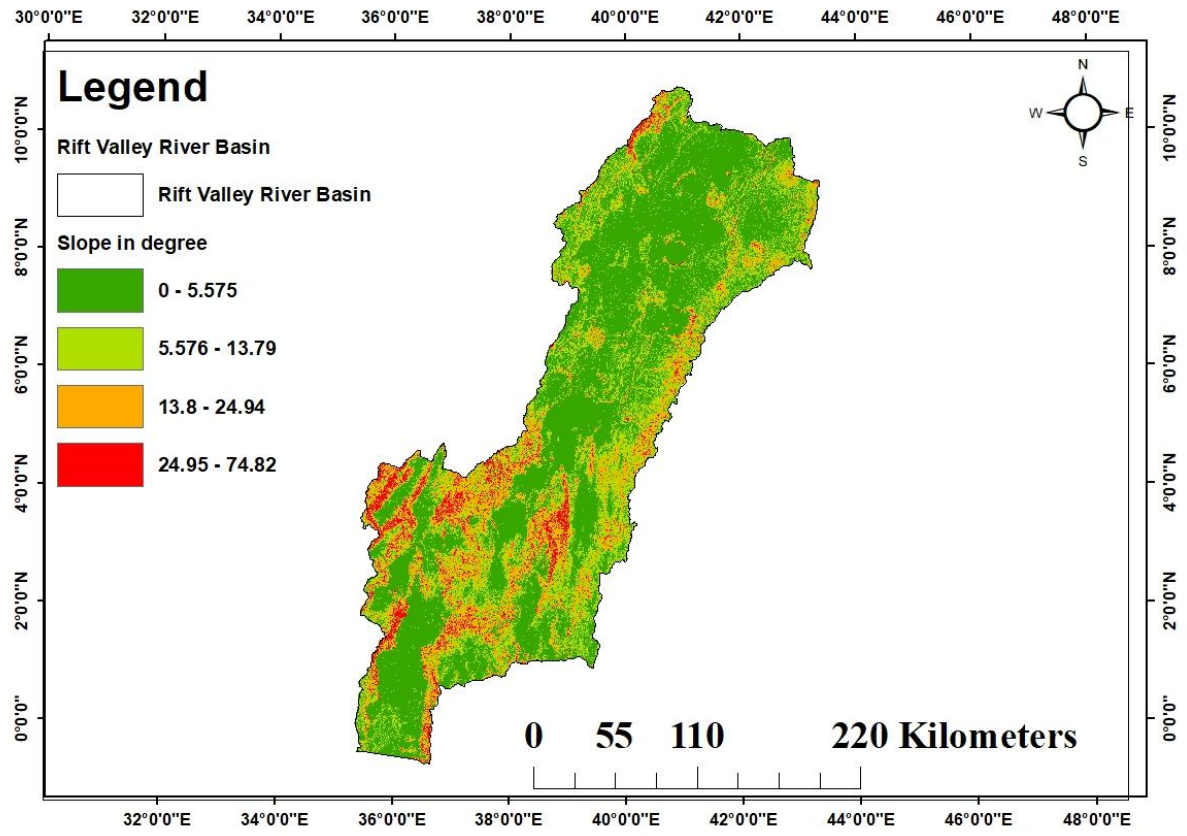

Figure 5 Slope characteristics of the Rift Valley basin.

2.2.4 Land Use Land Cover

Change in Land Cover and Land Use (LCLU) influences the runoff characteristics of a drainage basin to a large extent, affecting the area's surface and groundwater availability and hence leading to further change in LCLU. Therefore, the land use map is produced from the processing of the satellite Landsat 8OLI/TIRS USGS data (https://earthexplorer.usgs.gov, 2023) with a spatial resolution of 30 m, and the supervised classification is carried out to reclassify the land use land cover in the study area [65, 66]. After supervised classification, the accuracy of the image classification was analyzed using the confusion matrix of the spatial analysis tool ArcGIS 10.4. Classification accuracy was calculated using the Kappa value (K), which is a statistical coefficient that is used for the estimation of classification accuracy. According to Demir and Keshin [67], cited by Ayhan et al. [68], when the kappa value is 75% or more, the classification accuracy is considered to be very excellent; when it is between 40% and 75%, it is deemed to be medium-good; and when it is below 40%, it is considered to be weak. The estimated kappa value for this study area was 96%, which is very good and acceptable for further hydrological analysis. The land use and cover for the study area are presented in Figure 6. Also, land use changes occur constantly and at many scales. They can have specific and cumulative effects on air and water quality, watershed function, waste generation, wildlife habitat extent and quality, climate, and human health.

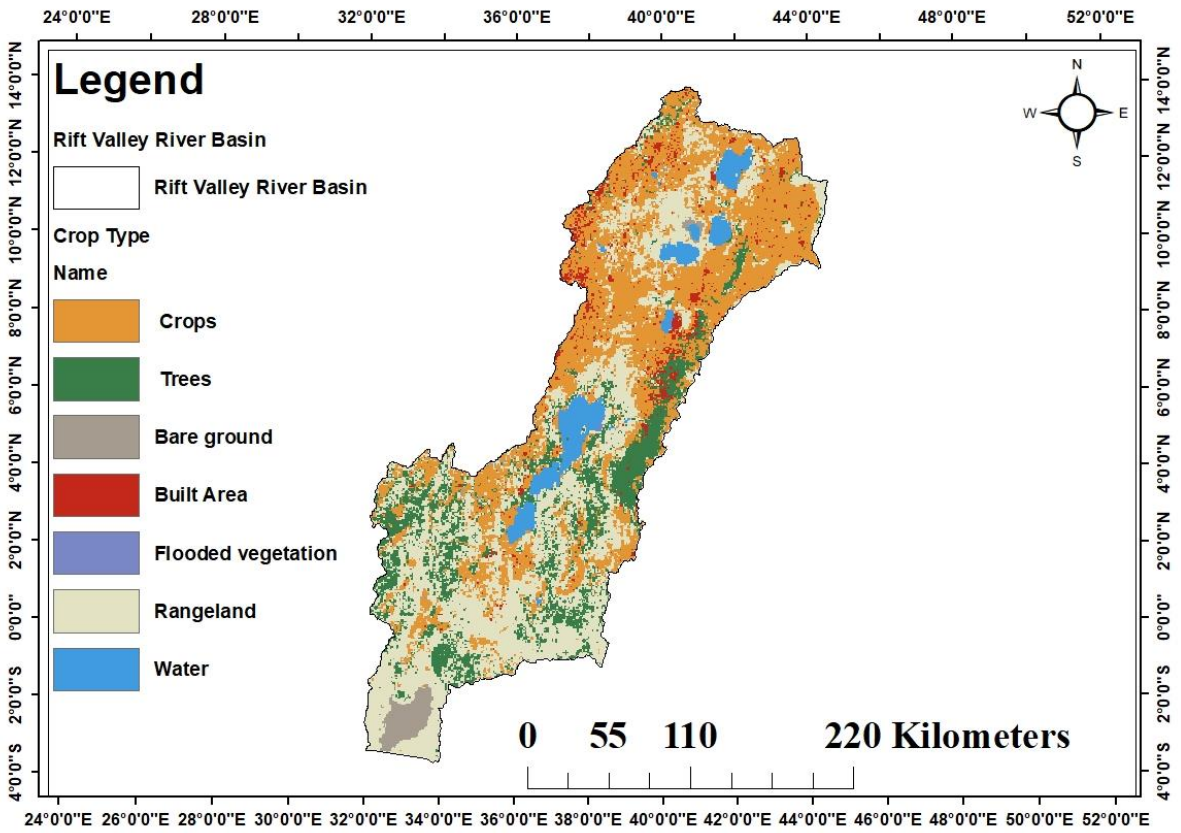

Figure 6 Land uses land cover characteristics in the Rift Valley basin.

2.2.5 Hydrological Soil Group

Any water that cannot immediately seep into the ground flows downslope as runoff. Ground permeability affects runoff significantly. Hard-packed clay soils might absorb very little water, while loose sand might absorb almost all the precipitation that falls onto them, resulting in virtually no runoff. So, the soil group affects rainfall runoff and is an important variable for the estimation of rainfall runoff [69]; therefore, the generation of runoff is controlled by soil characteristics, which are determined by the hydrological soil group with the parameters of soil texture, average clay content, soil depth, and infiltration rate. The hydrological soil group is obtained using soil data [70]. The characteristics of the soil texture with rainfall runoff, water transmission, and infiltration rate are presented in Table 1. Figure 7 shows the study area's hydrological soil group extracted from the world's FAO soil map, which has a 1:500,000 scale digital soil map and was converted to a raster dataset, projected, and reclassified based on the hydrological soil group. For the study area, we observed two hydrological soil groups.

Table 1 Soil conservation service classification (Source: [71]).

Hydrological soil group	Soil textures	Runoff potential	Water transmission	Final infiltration rate
Group A	Deep, well-drained sand and gravel	Low	High	>7.5
Group B	Moderately deep, well-drained, with moderate	Moderate	Moderate	3.8 to 7.5
Group C	Clay loam, shallow sandy loam, moderate to fine texture	Moderate	Moderate	1.3 to 3.8
Group D	Clay soils that swell significantly when wet	High	Low	<1.3

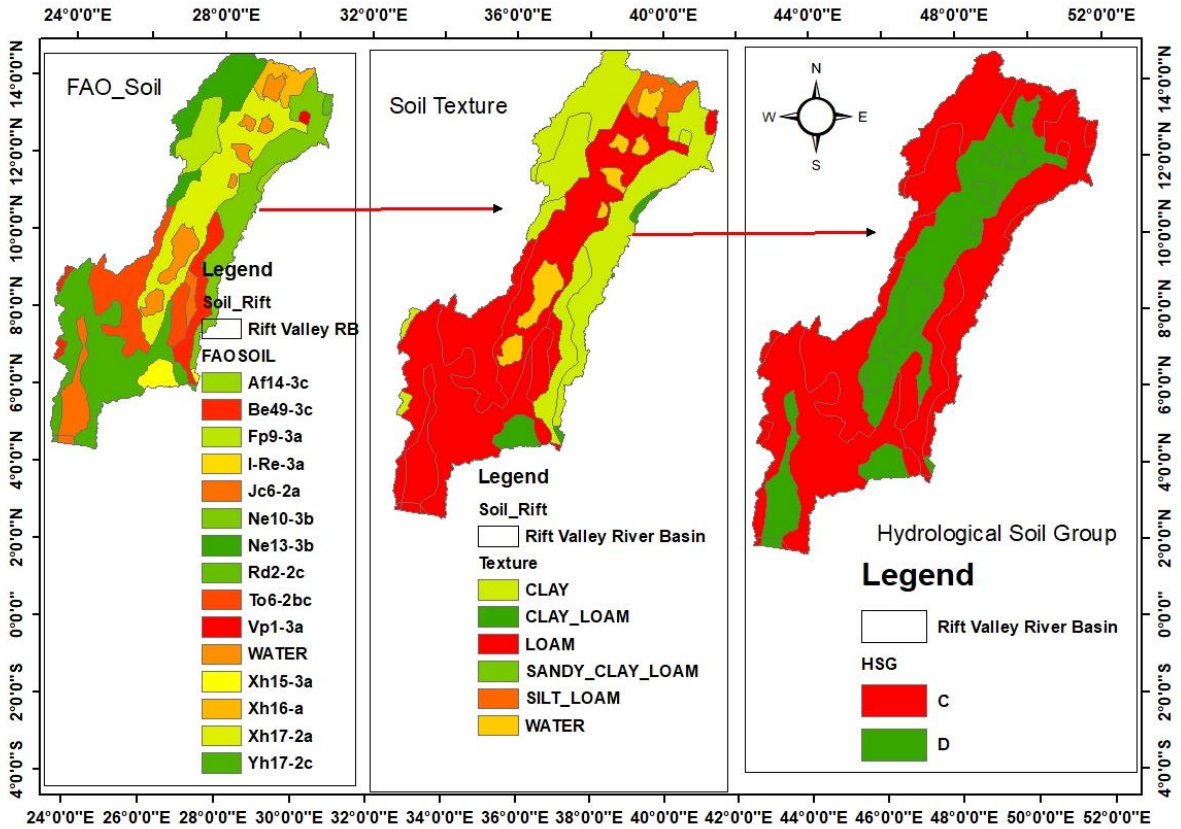

Figure 7 FAO soil type, soil texture, and hydrological soil group in the study area.

2.2.6 Antecedent Moisture Condition

Soil moisture is a key control for runoff generation and biogeochemical processes on hillslopes. Precipitation events can evoke different soil moisture responses with depth through the soil profile, and responses can differ among landscape positions along a hillslope. The antecedent moisture condition shows the water storage in the soil at a specified time when it is affected by total precipitation over the five days before the precipitation event [72]. Therefore, it is key in determining the maximum curve number value. However, the antecedent moisture condition value aims to show how the infiltration curves influence both the volume and the speed of surface runoff [73]. Generally,

SCS-CN shows three antecedent soil moisture situations and is represented as (I, II, and III) based on the change in soil condition and dormant and growth season rainfall amounts [74]. The antecedent soil moisture condition (I) shows the lowest surface runoff possibility due to sufficiently dry soils, whereas the antecedent soil moisture condition (II) represents the normal soil moisture condition, and the antecedent soil moisture condition (III) shows the highest surface runoff possibility. The curve number is determined by integrating the soil map and land use. So, this stage used antecedent moisture condition II, an average condition, to estimate the curve number value in the Rift Valley basin. The following equations (1) and (2) were used to calculate the values of curve numbers for antecedent soil moisture conditions I and III [75]:

$$CNI = \frac{4.2 \times CNII}{10 - 0.058 \times CNII} \quad (1)$$

$$CNIII = \frac{23 \times CNII}{10 + 0.13 \times CNII} \quad (2)$$

Where CNII is the curve number for everyday conditions, CNI is the curve number for dry conditions, and CNIII is the curve number for heavy rain and saturated soils. However, the SCS method was initially intended for 15-square-kilometer river basins. However, it has been altered to be used for bigger river basins by weighing curve numbers in relation to the river basins' land use areas [76]. The following equation (3) is used for the weighted curve number (CNw) [74]:

$$CN_w = \frac{\sum(CN_i \times A_i)}{A} \quad (3)$$

Where CN_w is the weighted cure number, CNi is the CN from 1 to any number, Ai is the area with the curve number CNi, and A is the total area of the river basin. The land use and HSG were combined using ArcGIS 10.4 software to produce a new polygon with a new attribute table. However, using the SCS-CN Tables, the CN was provided for each polygon depending on the properties of the land use and soil type, and equation 3 was applied to estimate the CNw for each land used in the Rift Valley basin. This method was also used by Matomela et al. [76] for the Tayiba Valley basin in Egypt. Table 2 shows the categorization of antecedent moisture condition

Table 2 Categorization of antecedent moisture condition (Sources: [71]).

AMC label	Assessment of soil condition	Total five-day antecedent rainfall(mm)	
		Dormant season	Growing season
I	The soil is dry, not to the point of withering	Less than 13	Less than 36
II	Normal condition	13 to 28	36 to 53
III	Heavy rains and saturated soils	Greater than 28	Greater than 53

2.2.7 SCS-CN Model

There are a number of models for calculating runoff, but the Soil Conservation Service Curve Number (SCS-CN), developed in 1954 by the USDA SCS [77], is the most popular empirical model for estimating rainfall runoff and is widely used [70], also called the Hydrological Soil Cover Complexes

Model [43]. This model is based on water balance estimation, which depends on two input variables: precipitation and curve number [78]. The soil conservation service curve number approach is frequently used empirically to estimate the direct runoff from a watershed [43]. Moreover, it also takes into account two primary presumptions. First, the ratio of surface runoff quantity to maximum rainfall is equal to the ratio of infiltration capacity to the volume of maximum retention. Secondly, the initial abstraction is one factor that could possibly result in maximum retention [40, 79]. The losses of infiltration are combined with external storage based on equation (4) [80].

$$Q = \frac{(P - I_a)^2}{P - I_a + S} \tag{4}$$

Where Q is surface runoff quantity, Ia is initial abstraction in mm before the onset of surface runoff and includes surface for storage, P is the depth of precipitation in mm, and S is the maximum possible retention after surface runoff in mm. The relationship between Ia and S is shown by equation (5) [81].

$$I_a = 0.2S \tag{5}$$

S can be obtained after knowing the CN; it is shown below by equation (6) [81].

$$S = \frac{25400}{CN} - 254 \tag{6}$$

The idea of CN is the curve number, which ranges from 0 to 100 [40] and is obtained from the table in accordance with the SCS manual of hydrology, relying on the land use and hydrological soil group consisting of four groups. Such as A, B, C, and D, antecedent soil moisture condition (AMC). So, the SCS curve number calculates how the soils allow water infiltration in relation to land use and antecedent soil moisture conditions [82]. Now, the equation can be rewritten as equation 7 below.

$$Q = \frac{(P - 0.3S)^2}{P + 0.7S} \tag{7}$$

Significantly higher the value of CN, the runoff from the watershed was calculated from the two equations above (6 and 7). Then, the rainfall runoff for the lake basin was calculated after estimating the necessary parameters.

2.2.8 water Management Using Rainfall-Runoff Modelling

The following Table 3 shows the related works for water management using rainfall-runoff modeling.

Table 3 Related works for water resource management using SCS-CN methods.

Kumari et al. [83]	Rainfall-runoff modeling using GIS-based SCS-CN method in Umiam catchment region, Meghalaya, India
Patel et al. [84]	Surface Runoff Estimation Using SCS-CN method- A Case Study on Bhadar Watershed, Gujarat, India
Reddy & Lalitha [85]	Rainfall-Runoff Analysis using Runoff Coefficient and SCS-CN Methods under GIS Approach.
Satheeshkumar et al. [40]	Rainfall-runoff estimation using SCS–CN and GIS approach in the Pappiredipatti watershed of the Vaniyar sub-basin, South India
Nandhakumar et al. [86]	Estimation of Rainfall-Runoff using Scs-Cn and Gis Approach in Puzhal Watershed, International Journal of Civil Engineering and Technology

3. Result

This study used the SCS-CN model for rainfall-runoff evaluation in the Rift Valley basin. The rainfall-runoff generation model is highly complex, nonlinear, dynamic in character, and affected by different interconnected physical factors. Hence, precise runoff estimation is carried out for valuable water resource management and development. In the Rift Valley River basin, drought-like situations prevail yearly due to low average annual precipitation and high runoff. The basin constitutes different land use land cover classes, and present studies show that rangeland is the dominant land use class, followed by cropland. In contrast, flood vegetation covers the lowest area in the study region. The built area and bare land play a crucial role in the rainfall runoff among the other land-use land cover types. The hydrological soil group also has important functionality in estimating the rainfall runoff potential and showing the soil character, category, and capability of infiltration rate. In this study, the hydrological soil groups A, B, C, and D were prepared based on the FAO soil map, geospatial data, and other secondary data. The obtained result shows that the C and D types of hydrological soil groups are mainly covered throughout the Rift Valley River basin. By overlay analysis of land use, land cover, and hydrological soil groups in the ArcGIS environment, the curve number values were assigned according to the USDA SCS, and the AMC values are AMC I, AMC II, and AMC III. The characteristics of precipitation, evapotranspiration, temperature, and soil moisture with rainfall runoff were evaluated.

3.1 Land Use Land Cover

The land use cover of our study is grouped into six land use types such as water bodies, trees, flooded vegetation, crops, built-up areas, bare land, and rangeland. As presented in Table 4 and Figure 6, the land use land cover map demonstrates that nearly 22763.82 km² (39.53%) of the Rift Valley basin area has been covered by rangeland, 19012.21 km² (30.01%) of the area is covered by cropland, 9003.65 km² (15.63%) is covered by trees, 3122.07 km² (5.42%) is covered by built-up areas, 2556.65 km² (4.44%) is covered by water bodies, 984.29 km² (1.71%) is covered by bare land, and 144.3 km² (0.25%) of the area is covered by flooded vegetation. One of the most crucial factors considered when estimating rainfall runoff is the type of land use, which significantly affects the pattern of rainfall runoff in any geographical region over time. This is because different types of land use affect a river basin differently, which also impacts its infiltration capacity and rate of rainfall

runoff, which agrees with similar findings [87, 88]. Areas with forest cover generally increase the infiltration rate and reduce rainfall runoff, whereas bare land surfaces or built areas increase rainfall runoff and lower the infiltration rate [87]. Recent studies conducted in Narok town revealed that land use and land cover change directly affect rainfall runoff intensity [89].

Table 4 Characteristics of land use land cover and its area coverage for the study area.

Type of land use land cover	Area	% area
Water	2556.65	4.44
Tree	9003.72	15.63
Flooded Vegetation	144.30	0.25
Crop	19012.21	33.01
Built Area	3122.07	5.42
Bare Land/cloud cover	984.29	1.71
Rangeland	22763.82	39.53
Sum	57587.08	100.00

3.2 Hydrologic Soil Group (HSG)

Soil has been grouped into four different hydrological soil classes, such as A, B, C, and D groups, according to infiltration rate, texture, water transmission capacity, drainage order, and transmissivity of water based on the USDA-SCS [90]. In this study, five textural soil classes were observed, such as clay, clay loam, loam, silty loam, and water, presented in Table 5 and Figure 7. As demonstrated in Table 4, the corresponding hydrological soil group has been assigned to each textural polygon, and two hydrological soil groups are identified using MWSWAT2012, i.e., C and D (Figure 7 and Table 4). The characteristics of the hydrological soil groups are specified regarding each soil group's reasonable infiltration rate, runoff potential, and water retention capacity in Table 4 based on USDA-SCS [87]. Surface runoff is generated when the movement of water into the soil is slow enough to result in water flow along the land surface and into water bodies. Areas with water bodies generally decrease the infiltration rate and increase rainfall-runoff, whereas regions with loam soil increase infiltration and reduce rainfall-runoff, consistent with previous studies [91].

Table 5 The characteristics of hydrological soil texture, hydrological soil group and area coverage.

FAOSOIL	DOMSOI	Hydrological soil group	Textural class	Area	% Area
Ne13-3b	Ne	C	Clay	4929.0	8.56
Xh16-a	Xh	C	Silty_Loam	277.0	0.48
Ne10-3b	Ne	C	Clay	4353.0	7.56
WATER	WR	D	Water	237.0	0.41
Xh17-2a	Xh	D	Loam	9748.0	16.93
Fp9-3a	Fp	C	Clay	2680.0	4.65
Vp1-3a	Vp	C	Clay	64.0	0.11
WATER	WR	D	Water	201.0	0.35

WATER	WR	D	Water	225.0	0.39
Be49-3c	Be	C	Clay	2073.0	3.60
WATER	WR	D	Water	318.0	0.55
Fp9-3a	Fp	C	Clay	16.0	0.03
Af14-3c	Af	C	Clay Loam	605.0	1.05
To6-2bc	To	C	Loam	5654.0	9.82
WATER	WR	D	Water	114.0	0.20
Be49-3c	Be	C	Clay	1960.0	3.40
WATER	WR	D	Water	1250.0	2.17
Ao39-2b	Ao	C	Loam	45.0	0.08
Yh17-2c	Yh	C	Loam	13886.0	24.11
Jc6-2a	Jc	D	Loam	527.0	0.92
To6-2bc	To	C	Loam	1087.0	1.89
WATER	WR	D	Water	510.0	0.89
Vc26-3a	Vc	D	Clay	65.0	0.11
Jc6-2a	Jc	D	Loam	2141.0	3.72
Xh15-3a	Xh	D	Clay Loam	4091.0	7.10
Jc6-2a	Jc	D	Loam	50.0	0.09
Jc6-2a	Jc	D	Loam	129.0	0.22
Yh17-2c	Yh	C	Loam	222.0	0.39
Jc6-2a	Jc	D	Loam	8.0	0.01
Yh17-2c	Yh	C	Loam	10.0	0.02
Rc22-2b	Rc	D	Loam	115.0	0.20
Total	-	-	-	57590.0	100.00

3.3 Curve Number (CN)

For this study, rainfall--runoff curve numbers have been taken from a hydrological modeling system [92]. The value of the curve number ranges from 0 to 100; a lower value shows low surface runoff with a high infiltration rate, whereas a higher value presents adequately higher rainfall runoff with a lower infiltration rate [93, 94]. For this study, the area curve number ranges from 74 to 80. The CN with low values is generally given to areas covered by trees, crops, and range land, whereas the CN with high values in the area is given to bare land, built areas, flooded areas, and water bodies. The different types of land use and land cover related to their respective hydrological soil groups and curve number values are presented in Table 6. Additionally, using equation 3, it has been found that the weighted curve number for the study area is 74.71, which is represented as AMC-II for normal soil moisture conditions. The curve numbers for AMC-I and AMC-III were calculated by equations 1 and 2, which give a result of 55.37 and 87.20, respectively, presented in Table 5. The rainfall-runoff curve number is an empirical variable used to calculate rainfall runoff in particular river basins, which agrees with similar studies [82, 95, 96].

Table 6 Distribution of land use land cover, hydrological soil group, and respective curve number values.

Type of land use land cover	Hydrological soil group	Curve Number	Area	% area	CN for AMCs
Tree	C	74	9003.72	15.63	**CNI = 55.37** **CNII = 74.71** **CNIII = 87.20**
Water	D	80	2556.65	4.44	
Crop	C	74	19012.21	33.01	
Flooded Vegetation	D	80	144.30	0.25	
Rangeland	C	74	22763.82	39.53	
Built Area	D	80	3122.07	5.42	
Bare Land/cloud cover	D	80	984.29	1.71	
Sum			57587.08	100.00	

After the CN value for each antecedent moisture content was evaluated, the probable maximum retention capacity (S) and preliminary abstraction loss (I_a) were estimated using equations 6 and 5, respectively. Their results are presented in Table 7.

Table 7 Estimation hydrological calculation for the Rift Valley basin (probable maximum retention, (S), preliminary abstraction loss (I_a) and CN_w).

	CN_w	S	$P > 0.2S = I_a$
AMC-I	55.37	213.73	42.75
AMC-II	74.71	94.98	19.00
AMC-III	87.20	46.38	9.28

3.4 Characteristics of Slope

For rainfall runoff estimation, the slope of an area is the foremost regulatory factor that determines the surface runoff and associated rate of infiltration capacity. Areas with a very steep slope permit a high rate of surface-runoff with a low infiltration rate, whereas areas with a gentle slope permit slow runoff with a high infiltration rate [97]. This study's topography is characterized by undulating, rugged, hilly terrain. The area's slope varies from 0 to 75.08 percent, as shown in Table 8. Figure 6 shows the slope map of the study area. Based on the characteristics of slope, a very low to high rate of runoff was estimated; i.e., slow runoff was estimated in areas with a low slope, whereas high runoff was estimated on the steepest slope of the hilly areas. 22.64 percent of the area was covered by nearly level terrain experiencing low rainfall-runoff, whereas 14.65 percent of the study area was covered by very steep sloping terrain experiencing very high rainfall runoff. The full details of rainfall runoff related to the characteristics of the slope in the area are presented in Table 7.

Table 8 Characteristics of the slope with landform and runoff.

Slope	Type of land form	Area in km^2	% Area	Relevancy of surface runoff
0 to 4.42	Nearly level	13026.40	22.64	Low rainfall runoff
4.43 to 10.31	Very gentle slope	15355.02	26.69	Moderate rainfall runoff
10.32 to 18.26	Gently sloping	11332.55	19.70	Moderate rainfall runoff
18.27 to 28.27	Moderate sloping	9393.09	16.33	high rainfall runoff
28.28 to 75.08	Strong sloping	8426.44	14.65	Very high rainfall runoff
Sum		57533.50	100.00	

3.5 Precipitation

Runoff is the proportion of rainfall that does not infiltrate and is not taken up by evapotranspiration. Precipitation serves as an important source of water and is one of the fundamental components of hydrology. However, the curve number method uses precipitation data to estimate river basin runoff and discharge [17]. Moreover, rainfall runoff creation is affected by the precipitation in the area. So, when precipitation is high, there is a corresponding increase in surface runoff. However, surface characteristics, like land use type and the textural class of the soil, can affect rainfall runoff directly or indirectly [56]. Hence, these values from 1991 to 2022 were collected from the climate forecast system reanalysis (CFSR): https://climatedataguide.ucar.edu/climate-data/climate-forecast-system-reanalysis-cfsr. The spatial variation of the precipitation for the study area is presented in Figure 3. Figure 3 shows a low spatial distribution of precipitation in the southern parts of the river basin, whereas high precipitation was observed in the same parts of the midstream section. Additionally, Fuka et al. [57] evaluated that the weather value generated by CFSR for river basin simulations is as good as or better than that used in simulations generated by conventional meteorological stations. The cumulative precipitation for this study is presented in Figure 8. Using multiple regressions, the statistical parameters of precipitation were evaluated. From the estimated result, the R-multiple is 0.11, the R-square value is 0.012, the adjusted R-square is -0.021, and the standard error is 119.13. The trend of precipitation shows rising and falling trends during the study period. The maximum yearly precipitation was observed in 2020 with a value of 1165.46 mm, followed by 1088.84 mm in 1997. In contrast, the minimum precipitation was observed in 2021 with a value of 673.22 mm, followed by 692.08 mm in 1999. The region's uneven precipitation results from changing weather patterns, which may bring more extreme weather events and lengthen drought and flood seasons, consistent with similar previous studies [1, 98].

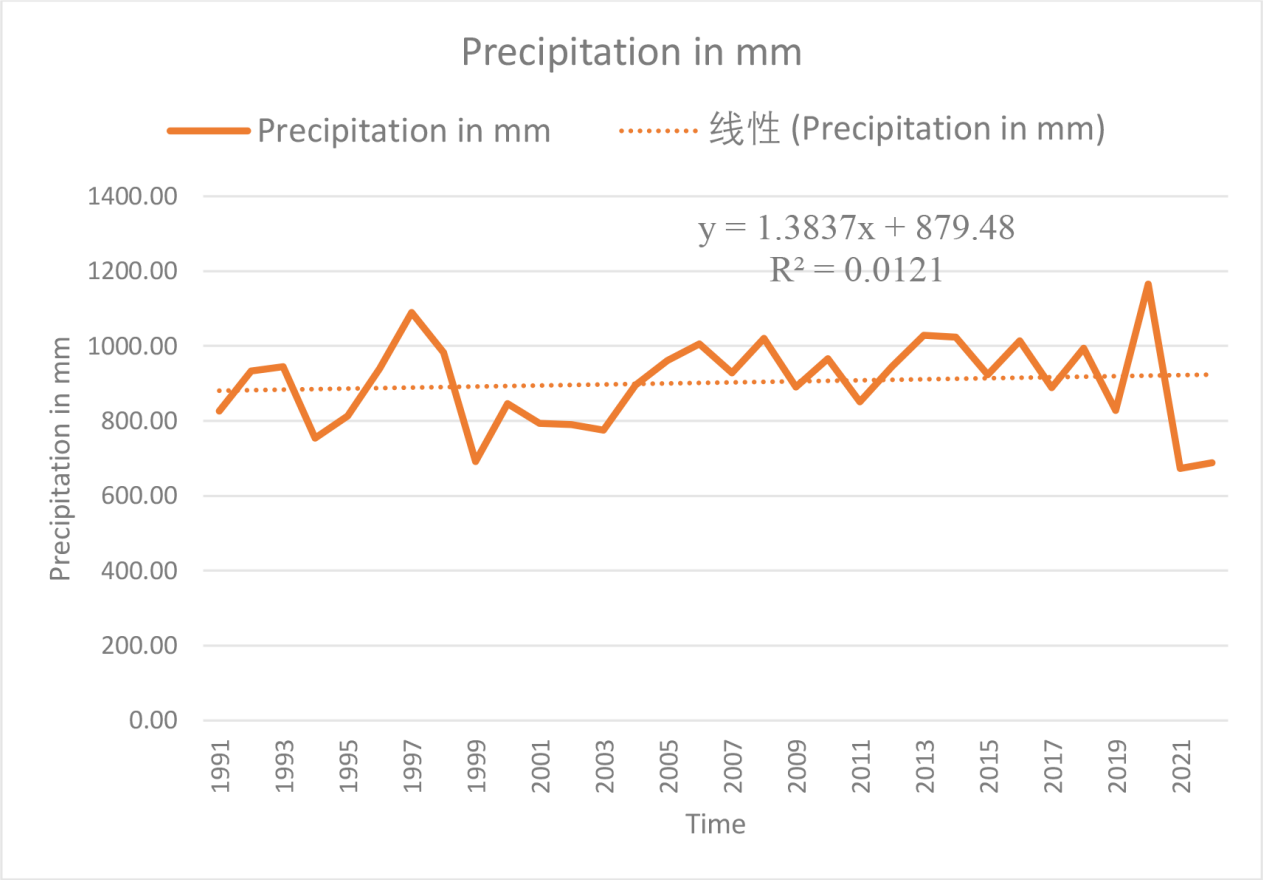

Figure 8 Annual precipitation for Rift Valley River basin from 1991 to 2021.

3.6 Estimation of Rainfall-Runoff for the Study Area

Using the available daily precipitation data from 1991 to 2021, the rainfall-runoff for the Rift Valley basin was calculated using equations 6 and 7 of the SCS-CN method. From the precipitation, we observed that the cumulative annual precipitation ranges from 673.22 to 1165.46 mm from 1991 to 2021, and the estimated average rainfall runoff varies between 562.70 and 1047.1 mm, as presented in Table 8. For the estimated result, the average volume of rainfall-runoff for the Rift Valley basin ranges from 32403589400 to 60303064900 Cubic Meters. The result in Table 8 shows cumulative precipitation, rainfall-runoff for AMC-I, II, and III, average rainfall runoff for the three-moisture condition, and the volume of rainfall-runoff for the study area. The correlation coefficient between precipitation and estimated rainfall runoff was 1, which shows precipitation was strongly correlated with rainfall runoff. This strong correlation shows that when precipitation increases, rainfall-runoff will also increase, and vice versa. The yearly rainfall-induced runoff rate is presented in Table 9. The result shows that maximum runoff occurred in 2020 with a value of 1047.11 mm, whereas the minimum rainfall runoff was observed in 2021 with a value of 562.66 mm.

Table 9 Estimated rainfall runoff for (AMC-I, II, III, average) in mm, Volume in cubic kilometers and cumulative precipitation in mm.

Year	Cumulative Precipitation in mm	Q for AMC-I = 54.96 in mm	Q for AMC-II = 74.39 in mm	Q for AMC-III = 86.98 in mm	Average rainfall runoff in mm	Volume in cubic meter
1991	827.12	623.75	732.19	783.89	713.28	41077795200
1992	934.00	726.51	838.19	890.59	818.43	47133383700
1993	945.21	737.33	849.32	901.78	829.48	47769753200
1994	754.17	554.16	659.97	711.09	641.74	36957806600
1995	812.63	609.88	717.84	769.43	699.05	40258289500
1996	939.93	732.24	844.08	896.51	824.28	47470285200
1997	1088.84	876.63	992.05	1045.23	971.30	55937167000
1998	983.09	773.96	886.93	939.61	866.83	49920739700
1999	692.08	495.38	598.61	649.15	581.05	33462669500
2000	847.04	642.83	751.93	803.77	732.84	42204255600
2001	793.99	592.08	699.38	750.82	680.76	39204968400
2002	791.03	589.26	696.45	747.87	677.86	39037957400
2003	775.67	574.61	681.24	732.54	662.80	38170652000
2004	894.82	688.74	799.31	851.47	779.84	44910985600
2005	961.05	752.64	865.05	917.60	845.09	48668733100
2006	1004.96	795.15	908.66	961.45	888.42	51164107800
2007	928.82	721.51	833.05	885.42	813.33	46839674700
2008	1020.60	810.32	924.21	977.07	903.86	52053297400
2009	890.33	684.42	794.86	846.99	775.42	44656437800
2010	965.71	757.15	869.68	922.25	849.69	48933647100
2011	850.35	646.01	755.22	807.08	736.10	42391999000
2012	944.24	736.40	848.36	900.82	828.52	47714466800
2013	1028.14	817.63	931.69	984.60	911.31	52482342900
2014	1023.81	813.43	927.39	980.27	907.03	52235857700
2015	923.33	716.22	827.60	879.94	807.92	46528112800
2016	1013.72	803.65	917.37	970.20	897.07	51662261300
2017	888.74	682.89	793.28	845.40	773.86	44566597400
2018	994.95	785.45	898.72	951.45	878.54	50595118600
2019	827.99	624.58	733.06	784.76	714.13	41126746700
2020	1165.46	951.32	1068.26	1121.76	1047.11	60303064900
2021	673.22	477.62	580.00	630.35	562.66	32403589400
2022	688.96	492.44	595.53	646.04	578.00	41077795200

The long-term temporal variation of rainfall runoff for the study area shows rising and falling trends for the study durations. The variation in rainfall-runoff for the study area was observed due to the variation in precipitation caused by climatic change and greed, with similar previous findings [6, 35, 98]. Figure 9 demonstrates the temporal variation of rainfall runoff in the Rift Valley basin from 1991 to 2022.

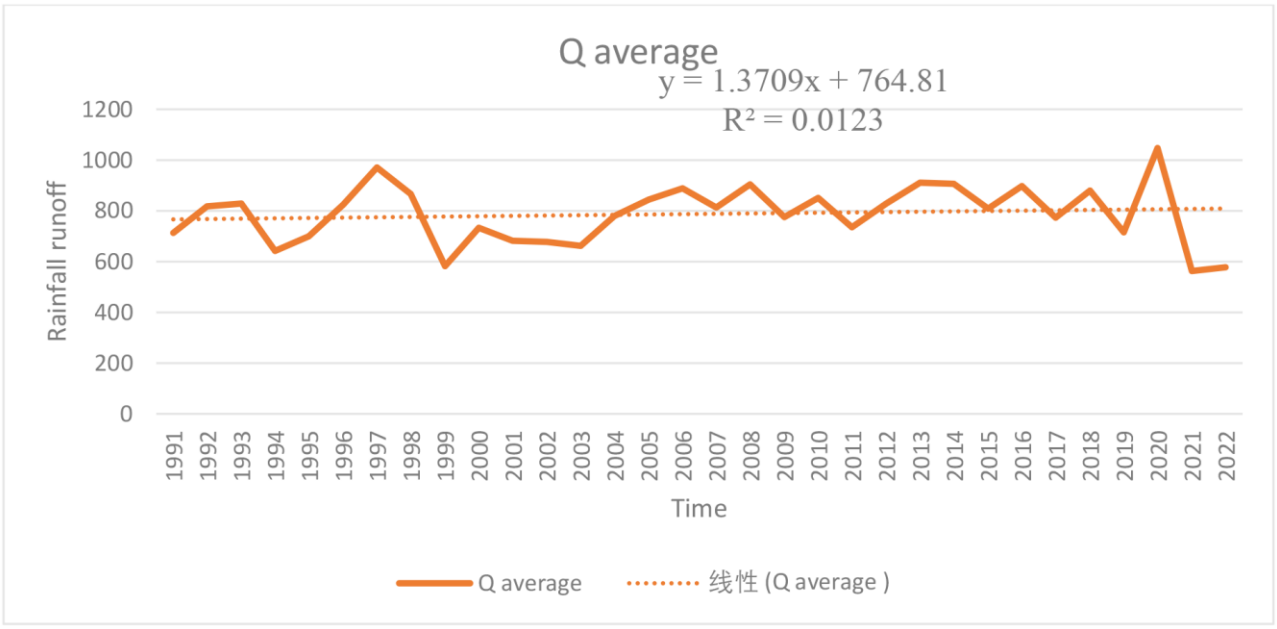

Figure 9 Estimated average rainfall-runoff characteristics in the Rift Valley basin.

3.7 Spatial Distribution of Rainfall-Runoff in Rift Valley Basin

The estimated spatial distribution of rainfall runoff in the Rift Valley basin from 2011 to 2022 is presented in Figure 10. As presented in Figure 10, the low spatial distribution of rainfall-runoff has been observed in the downstream sections of the river basin for the entire year. As shown in Figure 10, most of the river basin experiences low rainfall-runoff, whereas a few parts of the river basin experience high rainfall runoff. As indicated in Figure 10, the rainfall-runoff of the river basin ranges from 1.25 to 71.75 mm in 2011, 2.08 to 66.67 mm in 2012, 2.08 to 74.25 mm in 2013, 1.5 to 78.5 mm in 2014, 1.5 to 64.33 mm in 2015, 1.33 to 62.08 mm in 2016, 1.58 to 56.92 mm in 2017, 2.08 to 72.83 mm in 2018, 1.33 to 57.5 mm in 2019, 1.92 to 100.7 mm in 2020, 0.83 to 38.08 mm in 2021, and 0.67 to 29.83 mm in 2022. As presented in Figure 10, the lowest rainfall runoff was observed in 2022, with a value range of 0.67 to 29.83 mm, whereas the highest rainfall runoff was observed in 2020, with a value range of 1.92 to 100.7 mm. As observed in Figure 10, the variation in rainfall-runoff for this study is due to land use, land cover, soil type, anthropogenic activities, and climatic change, consistent with similar previous studies. A similar result was achieved by Umukiza et al. [89], who demonstrated how the configuration and composition of land use can affect rainfall runoff and flow volume in selected catchments of Narok Town, Kenya.

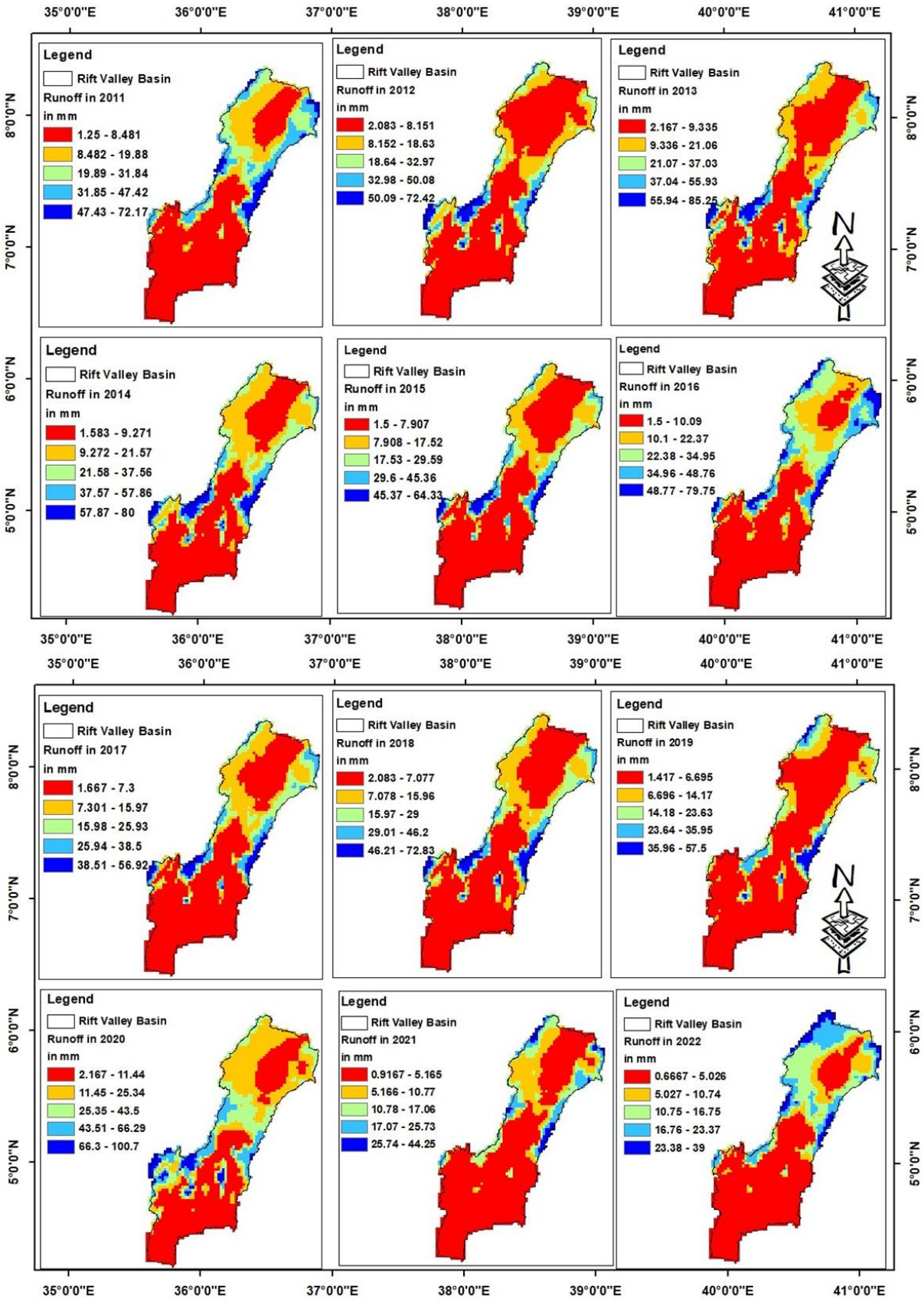

Figure 10 Spatial distribution of rainfall runoff in the Rift Valley basin from 2011 to 2022.

4. Discussions

4.1 Relationship between Precipitation, Evapotranspiration, Temperature, and Rainfall Runoff

Figure 11 presents the relationship between rainfall-runoff, precipitation, evapotranspiration, and temperature. As indicated in Figure 11, precipitation and rainfall runoff follow a similar trend. As precipitation is the source of the hydrological cycle, increasing precipitation leads to increasing rainfall runoff, and decreasing precipitation leads to decreasing rainfall runoff, which shows a direct relationship that agrees with previous similar studies [1, 99, 100]. As demonstrated in Figure 11, the relationship between evapotranspiration and rainfall runoff shows significant and varying trends. As observed in Figure 11, at certain times, evapotranspiration and rainfall runoff show a similar trend. Still, at other times, they show variation in trend, which depends on the seasonal variation of the environment. During the rainy season, the effect of evapotranspiration on rainfall-runoff is insignificant. Still, during the dry season, the effect of evapotranspiration is high. We agreed that a similar trend was observed during the wet season due to the low impact of evapotranspiration on rainfall-runoff. In contrast, a varying trend is observed during dry and drought conditions, confirmed by similar previous studies [101]. As presented in Figure 11, increasing temperature leads to a decrease in rainfall-runoff, and a reduction in temperature leads to an increase in rainfall runoff. This is due to climatic change and is confirmed by similar findings [1, 102]. As presented in Figure 11, the relationship between soil moisture and rainfall runoff shows a similar trend. As soil moisture increases, the rainfall-runoff in an area also increases, which agrees with previous studies [103].

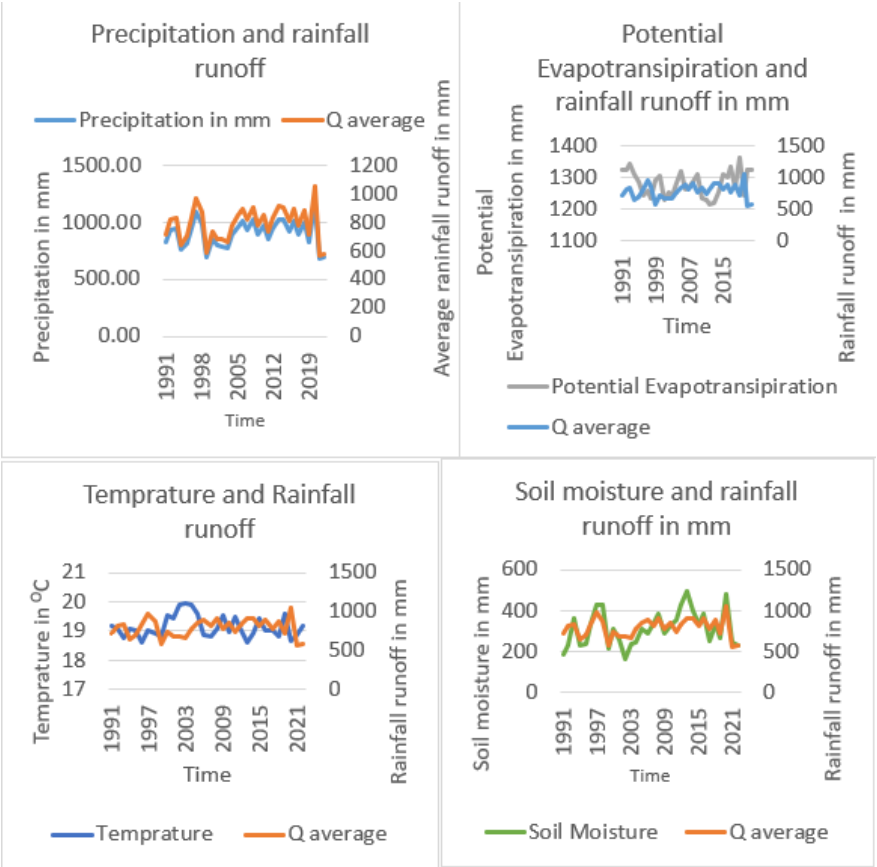

Figure 11 Relationship between precipitation, soil moisture, evapotranspiration and temperature with rainfall runoff.

Understanding the hydrological behaviors of river basins is an important part of effective river basin management and planning. In this study, rainfall-runoff modeling is carried out using CN-SCN methods in the Rift Valley basin for water resource management and optimal utilization. Different datasets are collected and utilized to evaluate rainfall runoff for the study area, like precipitation, land use, land cover, slope data, and soil datasets. As presented in Figure 6, the land use cover of the study area is classified into seven classes: rangeland, bare ground, water bodies, trees, flooded vegetation, crops, and built area. A comprehensive understanding of the impact of land use and land cover change, especially on hydrology, is important for developing sustainable water resource management strategies that optimize economic and social welfare without jeopardizing ecosystem sustainability. The impact of land use and land cover change on hydrological responses is critical and also presented by other findings [104-106]. As presented in Table 4, the study area covered 4.44 percent by water, 15.63 percent by tree, 0.25 percent by flood vegetation, 33.01 percent by crop, 5.42 percent by built area, 1.71 percent by bare land, and 39.53 percent by rangeland. Recent studies in Narok town revealed that land use and land cover change directly affect rainfall runoff intensity [6]. As presented in Figure 7, the hydrological soil groups of the study area are grouped into C and D, with five textural classes (clay, clay loam, loam, silty loam, and water). Soil physical characteristics affect water infiltration rate into the soil and influence rainfall runoff in any area. Surface runoff is generated when the soil is saturated. In clay soil, rainfall-runoff is higher than in sandy soil due to the permeability of the soil porosity, which allows the downward movement of water to recharge groundwater and reduce rainfall runoff. A similar result was reported by Chen[107] in hillslope cropland of purple soil in China. They reported that sand, loam sand, and sandy loam have a minimum infiltration rate of more than 7.26 mm per hour, whereas clay and silty clay have a minimum infiltration rate range of 0 to 1.24, which affects rainfall runoff. Table 5 and Figure 7 show that the study area accounts for 34.26 percent of the D hydrological soil group and 65.74 percent of the C hydrological soil group. On land, surface precipitation is one of the most natural resources for obtaining fresh water and creating rainfall runoff. It is an essential part of the hydrological cycles, and for the study area, the spatial distribution of precipitation ranges from 31.69 to 142.5 mm and the year precipitation ranges from 673.22 to 1165.46 mm, as presented in Figure 3 and Figure 8, respectively, which are important parameters for the estimation of the spatial and yearly variation of rainfall runoff in the study area. As presented in Figure 3, some parts of the river basin in the midstream section are experiencing very high precipitation, the southern parts are experiencing very low precipitation, and the rest are experiencing medium to low precipitation. As precipitation increases, the rainfall-runoff also increases, whereas as precipitation decreases, the rainfall runoff also decreases, which is also reported by similar previous studies [1, 108-110]. Soil moisture before rainfall will significantly affect the rainfall-runoff capacity and CN values of the area because it can check and balance the infiltration rate and quantity of moisture. Considering the effects, using a 5-day antecedent precipitation index, we evaluated the antecedent soil moisture content for dry, normal, and wet conditions, and the results are presented in Table 5. As presented in Table 5, the CN for AMCI is 55.37, AMCII is 74.71, and the CNIII for AMCIII is 87.20. The CN with low values is generally given for areas having crops, trees, and rangeland; however, the CN with high values is for built areas, bare land, water bodies, and flooded areas due to its contribution of rainfall runoff, which agrees with previous studies [1, 111]. As presented in Table 7, the probable maximum retention capacity and preliminary abstraction loss were evaluated to estimate rainfall runoff for the study area. Maximum potential retention represents the maximum amount of water in mm retained on

the watershed surface after rainfall runoff begins. This is an important variable in the CN-SCS method of runoff estimation. It is not a directly measurable watershed variable. Preliminary abstraction loss is a parameter that accounts for all losses before runoff and consists mainly of interception, infiltration, evaporation, and surface depression storage. In theory, all rainfall minus preliminary abstraction loss will generate the runoff from a specified river basin. As presented in Table 7, the maximum probable retention for AMC-I is 213.73, AMC-II is 94.98, and AMC-III is 46.38, whereas the preliminary abstraction loss is 42.75 for AMC-I, 19.0 for AMC-II, and 9.28 for AMC-III. As shown in Table 7, the maximum value of maximum probable retention and abstraction losses were observed for AMC-I. This is because before rainfall runoff begins, it balances the soil moisture condition in the soil and maximum infiltration and decreases as precipitation increases, which agrees with similar findings [99, 110]. The slope is an important parameter that affects rainfall runoff. As the slope of the area increases, infiltration decreases with increasing rainfall-runoff, whereas decreasing the land surface slope increases the soil infiltration rate and reduces rainfall runoff. As presented in Table 7 and Figure 6, the slope of the study area ranges from 0 to 75.08 percent. As demonstrated in Table 7, 22.64 percent of the study area slope ranges from 0 to 4.42 with nearly level rainfall-runoff, 26.69 percent of the area slope ranges from 4.43 to 10.31 with a very gentle slope having moderate rainfall-runoff, 19.7 percent of the area slope ranges from 10.32 to 18.26 percent with gently sloping having moderate rainfall-runoff, 16.33 percent of the study area slope ranges from 18.27 to 28.27 with moderate sloping with high rainfall runoff, and 14.65 percent of the area slope ranges from 28.28 to 75.08 with strong sloping creating very high rainfall runoff. We understand that under the condition of equal horizontal projective lengths so that all slopes receive the same amount of rainfall, there are increases in infiltration with increasing slope gradients and decreasing rainfall runoff, and the steeper the slopes, the faster the rainfall-runoff, which is consistent with similar studies [1, 99, 110, 112].

For this study, soil conservation service curve number rainfall runoff was generated based on precipitation, abstraction loss, and probable maximum soil retention potential, and these datasets are used as input for the ArcGIS-based SCS-CN rainfall-runoff simulation model. As presented in Table 8, the estimated rainfall runoff ranges from 562.70 to 1047.10 mm, and the temporal variation of rainfall-runoff during this study period is observed due to changes in precipitation and climatic change, which agrees with previous similar studies [1, 98]. As presented in Figure 10, the spatial distribution of rainfall-runoff ranges from 0.67 to 100.7 mm during the study period, and the variability of this spatial distribution of rainfall runoff is observed due to the variability of precipitation across the study area. The curve number resulted from land use, land cover, hydrological soil group, anthropologic activity, and climatic change, which agrees with similar previous findings [98, 113, 114]. Rainfall-runoff estimation from a river basin is used to develop hydraulic structures, regulate soil erosion, analyze the water supply potential of a river basin, and develop groundwater recharge by collecting rainfall runoff in artificial recharge areas. The SCS-CN method is probably a very well-defined and straightforward conceptual model for calculating rainfall runoff from precipitation. Therefore, in the current study, we utilized the SCS-CN method to estimate rainfall runoff in a drought-prone area of the Rift Valley basin, relying on the daily precipitation from the basin for 31 years, i.e., 1991–2022, where the SCS-CN method is the most popular for estimating the volume of rainfall-runoff for a certain precipitation event, and this method offers more dependability. It is a fact that the SCS-CN model has been widely used across the globe under different land use, land cover, and climatic conditions to evaluate rainfall runoff since its

development [75, 115, 116]. Although this model has been used for a range of applications outside of its initial focus, such as rainfall-runoff analysis in vast river basins and integration into daily and long-term hydrological models [117, 118]. Different researchers have done their work using the SCS-CN method to calculate rainfall runoff, and their output is optimal for sustainable watershed management [31, 38, 75, 119]. Also, currently, machine learning and various approaches have been used to calculate rainfall runoff in the natural river basin [19, 107, 120-121]. As the SCS-CN is primarily affected by precipitation, land use, land cover, hydrological soil group, and antecedent soil moisture condition, all of these variables are utilized as input variables for the estimation of rainfall-runoff by the SCS-CN method to create and evaluate the weighted curve number in the Rift Valley basin. In this undulating drought-prone watershed, the rainfall-runoff is robustly correlated with an R-value of 1. Therefore, there is high seasonal precipitation during the wet season (April to September), and the lowest rainfall runoff is estimated in the dry season for the study area from November to February. Figure 12 shows the rainfall-runoff characteristics for the three antecedent moisture conditions with precipitation in the study area. The estimated rainfall runoff for the study area is directly related to the precipitation in the area. As presented in Figure 10, the spatiotemporal variation of the rainfall-runoff in the Rift Valley basin shows significant variation during the study period. As shown in Figure 10, the majority of the study area experiences very low rainfall-runoff, whereas very few parts of the study area demonstrate very high rainfall runoff. As indicated in Figure 10, the rainfall-runoff of the river basin ranges from 1.25 to 71.75 mm in 2011, 2.08 to 66.67 mm in 2012, 2.08 to 74.25 mm in 2013, 1.5 to 78.5 mm in 2014, 1.5 to 64.33 in 2015, 1.33 to 62.08 mm in 2016, 1.58 to 56.92 mm in 2017, 2.08 to 72.83 in 2018, 1.33 to 57.5 mm in 2019, 1.92 to 100.7 mm in 2020, 0.83 to 38.08 mm in 2021, and 0.67 to 29.83 mm in 2022. As presented in Figure 10, the lowest rainfall runoff is observed in 2022, with a value range of 0.67 to 29.83 mm, whereas the highest rainfall runoff is observed in 2020, with a value range of 1.92 to 100.7 mm. As observed in Figure 10, the variation in rainfall-runoff for this study is due to land use, land cover, soil type, anthropogenic activities, and climatic change, consistent with similar previous studies. A similar result was achieved by Umukiza et al. [89], who demonstrated how the configuration and composition of land use can affect rainfall runoff and flow volume in selected catchments of Narok Town, Kenya. The relationship between precipitation, evapotranspiration, soil moisture, and temperature with rainfall runoff was evaluated. As presented in Figure 11, precipitation and soil moisture show a similar trend with rainfall-runoff, whereas evapotranspiration and temperature show a significant and varying trend with rainfall-runoff. The variation of rainfall-runoff is mostly observed due to the variability of precipitation, temperature, and other climatic parameters, consistent with similar previous findings [1, 99-101, 103, 122].

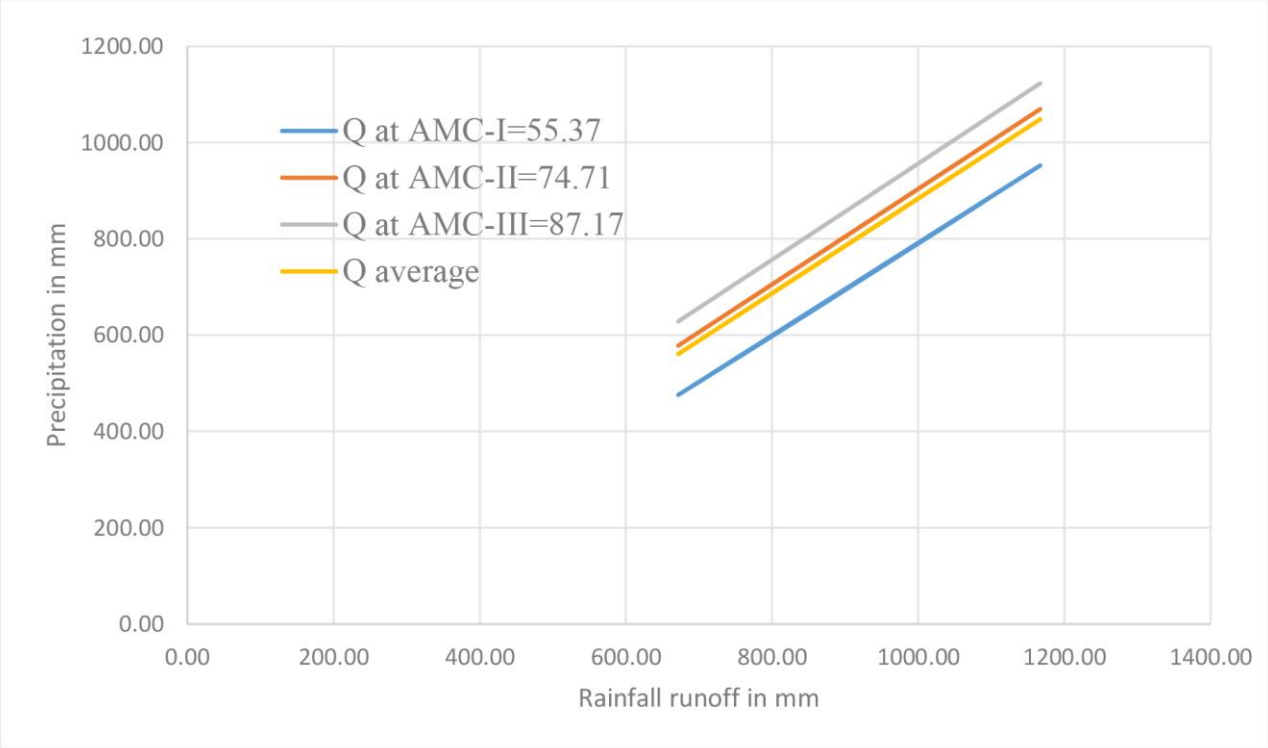

Figure 12 Characteristics of rainfall runoff with precipitation for AMC-I, II, and III in Rift Valley basin.

5. Conclusion

This paper investigates the characteristics of rainfall runoff in the Rift Valley basin using the SCS-CN method with integrated ArcGIS, which can effectively be used in water resource management. The land use, land cover, soil data, slope, and precipitation data were used to evaluate rainfall runoff in the Rift Valley basin. For the generated land use, land cover, and hydrological soil group, antecedent moisture conditions for wet, normal, and dry conditions were evaluated, which were equal to 54.96 for AMC-I, 74.39 for AMC-II, and 86.98 for AMC-III. In addition to the curve number, probable maximum retention and preliminary abstraction loss for the estimated curve number were evaluated. The estimated probable maximum retention is 213.73, 94.98, and 46.38 for AMC-I, II, and III, respectively, whereas the preliminary abstraction loss is 42.75, 19.00, and 9.28 for AMC-I, II, and III, respectively. The estimated average rainfall runoff in the Rift Valley basin varies between 562.70 and 1047.1 mm, with an average volume of 32403589400 to 60303064900 Cubic Meter from 1991 to 2021. The spatiotemporal characteristics of rainfall runoff in the Rift Valley basin are also evaluated, and the results range from 0.67 to 100.7 mm. The characteristics of precipitation, temperature, soil moisture, and evapotranspiration with rainfall runoff are evaluated in the study area. In addition to that, this study highlights the importance of using SCS-CN GIS-based methods and GIS and remote sensing data. So, the GIS SCS-CN method merged with remote sensing, was utilized to calculate surface runoff in the Rift Valley basin. Hence, the rainfall runoff depth and volume in the Rift Valley basin will provide surface water availability. In addition, the potential is important for various uses, such as domestic water supply, irrigation, and power production in the area, as well as the construction and design of drains, bridges, and others. In conclusion, the Soil Conversations Service-Curve Number approach is efficiently proven to be a better method, which

consumes less time and has the facility to handle an extensive data set and a larger environmental area to identify the site selection of artificial recharge structures.

Sedimentation affected the Lake Chamo water body, and our work's future prospect was to evaluate sedimentation for effective water resource management and ecological restoration.

Abbreviations

SCS-CN	Soil Conservation Service Curve Number
GIS	Geographic Information System
SWAT	Soil and Water Assessment Tool
SHE	Systeme Hydrologique Europeen
HEC-HMS	Hydrologic Engineering Center-Hydrologic Modeling System
TRMM	Tropical Rainfall Measuring Mission
IRS	Infiltration and Runoff Simulation
NOAA	National Oceanic and Atmospheric Administration
DEM	Digital elevation model
RS	Remote Sensing
LULC	Land use land cover
USGS	United States Geological Survey
MODIS	Moderate Resolution Imaging Spectroradiometer
CHIRPS	Climate Hazards Group InfraRed Precipitation
CFSR	Climate Forecast System Reanalysis
FAO	Food and Agriculture Organization
AMC	Antecedent Moisture Condition
HSG	Hydrologic Soil Group

Author Contributions

Conceptualization, methodology, original draft writing, preparation, and development of model was curried by the A. K. Yoshe.

Funding

This research did not receive any specific grant from funding agencies in the public, commercial or non-profit sectors.

Competing Interests

The author declares no competing interests.

Data Availability Statement

The dataset utilized for the estimation of rainfall runoff during this study are available from the corresponding author on reasonable request.

References

1. Bera A, Taloor AK, Meraj G, Kanga S, Singh SK, Đurin B, et al. Climate vulnerability and economic determinants: Linkages and risk reduction in Sagar Island, India; A geospatial approach. Quat Sci Adv. 2021; 4: 100038.
2. Mondal M, Biswas A, Haldar S, Mandal S, Mandal P, Bhattacharya S, et al. Climate change, multi-hazards and society: An empirical study on the coastal community of Indian Sundarban. Nat Hazards Res. 2022; 2: 84-96.
3. Shumilova O, Tockner K, Sukhodolov A, Khilchevskyi V, De Meester L, Stepanenko S, et al. Impact of the Russia–Ukraine armed conflict on water resources and water infrastructure. Nat Sustain. 2023; 6: 578-586.
4. Kumar P, Tokas J, Kumar N, Lal M, Singal HR. Climate change consequences and its impact on agriculture and food security. Int J Chem Stud. 2018; 6: 124-133.
5. Ahmad D, Afzal M. Flood hazards, human displacement and food insecurity in rural riverine areas of Punjab, Pakistan: Policy implications. Environ Sci Pollut Res. 2021; 28: 10125-10139.
6. Yamamoto K, Sayama T, Apip. Impact of climate change on flood inundation in a tropical river basin in Indonesia. Prog Earth Planet Sci. 2021; 8: 5.
7. Nguyen TT, Ngo HH, Guo W, Wang XC, Ren N, Li G, et al. Implementation of a specific urban water management-Sponge City. Sci Total Environ. 2019; 652: 147-162.
8. Leahy SM, Robins JB. River flows affect the growth of a tropical finfish in the wet-dry rivers of northern Australia, with implications for water resource development. Hydrobiologia. 2021; 848: 4311-4333.
9. Ojile MO, Ogwara EO. Vulnerability of communities to flood hazard and riverbank erosion along River Nun in Bayelsa State, Nigeria. Glob J Adv Eng Technol Sci. 2022; 9: 1-8.
10. Golshan M, Ebrahimi P. Estimation of the Runoff by empirical equations in dry and mid-dry mountainous area without stations (Case Study: Madan Watershed, Qazvin Province-Iran). Bull Environ Pharmacol Life Sci. 2014; 3: 77-85.
11. Pérez-Sánchez J, Senent-Aparicio J, Segura-Méndez F, Pulido-Velazquez D, Srinivasan R. Evaluating hydrological models for deriving water resources in peninsular Spain. Sustainability. 2019; 11: 2872.
12. Niharika S, Panigrahi B, Mohan DD, Das DP. Simulation of runoff in Baitarani basin using composite and distributed curve number approaches in HEC-HMS model. Mausam. 2020; 71: 675-686.
13. Choudhari K, Panigrahi B, Paul JC. Simulation of rainfall-runoff process using HEC-HMS model for Balijore Nala watershed, Odisha, India. Int J Geomat Geosci. 2014; 5: 253-265.
14. Nayak TR, Jaiswal RK. Rainfall-runoff modelling using satellite data and GIS for Bebas river in Madhya Pradesh. J Inst Eng India Civil Eng Div. 2003; 84: 47-50.
15. Beven KJ. Rainfall-runoff modelling: The primer. Hoboken, NJ: John Wiley & Sons; 2011.
16. Devia GK, Ganasri BP, Dwarakish GS. A review on hydrological models. Aquat Procedia. 2015; 4: 1001-1007.
17. Anshuka A, van Ogtrop FF, Willem Vervoort R. Drought forecasting through statistical models using standardised precipitation index: A systematic review and meta-regression analysis. Nat Hazards. 2019; 97: 955-977.

18. Chen L, Young MH. Green-Ampt infiltration model for sloping surfaces. Water Resour Res. 2006; 42: W07420.
19. Tsykin EN. Multiple nonlinear statistical models for runoff simulation and prediction. J Hydrol. 1985; 77: 209-226.
20. Todini E. Rainfall-runoff modeling—Past, present and future. J Hydrol. 1988; 100: 341-352.
21. Madsen H. Automatic calibration of a conceptual rainfall–runoff model using multiple objectives. J Hydrol. 2000; 235: 276-288.
22. Sherman LK. The unit hydrograph method. In: Physics of the Earth. New York, NY: McGraw-Hill; 1949. pp. 514-525.
23. Mockus V. Estimation of total surface runoff for individual storms. Exhibit A of Appendix B—Interim Survey Report Grand (Neosho) River Watershed. Washington, DC: United States Department of Agriculture; 1949.
24. Musgrave GW. How much of the rain enters the soil? In: Water: Yearbook of agriculture. Washington, DC: United States Department of Agriculture; 1955.
25. Woodward DE, Hawkins RH, Quan QD. Curve number method: Origins, applications and limitations. Proceedings of the 2nd Federal Interagency Hydrologic Modeling Conference; 2002 July 28-August 1; Las Vegas, NV, USA.
26. Fu S, Zhang G, Wang N, Luo L. Initial abstraction ratio in the SCS-CN method in the Loess Plateau of China. Trans ASABE. 2011; 54: 163-169.
27. Verma S, Verma RK, Mishra SK, Singh A, Jayaraj GK. A revisit of NRCS-CN inspired models coupled with RS and GIS for runoff estimation. Hydrol Sci J. 2017; 62: 1891-1930.
28. Arnold JG, Allen PM. Estimating hydrologic budgets for three Illinois watersheds. J Hydrol. 1996; 176: 57-77.
29. Anderson ML, Chen ZQ, Kavvas ML, Feldman A. Coupling HEC-HMS with atmospheric models for prediction of watershed runoff. J Hydrol Eng. 2002; 7: 312-318.
30. Romero P, Castro G, Gómez JA, Fereres E. Curve number values for olive orchards under different soil management. Soil Sci Soc Am J. 2007; 71: 1758-1769.
31. Soulis KX, Valiantzas JD. Identification of the SCS-CN parameter spatial distribution using rainfall-runoff data in heterogeneous watersheds. Water Resour Manag. 2013; 27: 1737-1749.
32. Garg V, Nikam BR, Thakur PK, Aggarwal SP, Gupta PK, Srivastav SK. Human-induced land use land cover change and its impact on hydrology. HydroResearch. 2019; 1: 48-56.
33. Schultz GA. Remote sensing in hydrology. J Hydrol. 1988; 100: 239-265.
34. Williams JR, LaSeur WV. Water yield model using SCS curve numbers. J Hydraul Div. 1976; 102: 1241-1253.
35. Voda M, Sarpe CA, Voda AI. Romanian river basins lag time analysis. The SCS-CN versus RNS comparative approach developed for small watersheds. Water Resour Manag. 2019; 33: 245-259.
36. Verma S, Singh PK, Mishra SK, Singh VP, Singh V, Singh A. Activation soil moisture accounting (ASMA) for runoff estimation using soil conservation service curve number (SCS-CN) method. J Hydrol. 2020; 589: 125114.
37. Khaddor I, Achab M, Soumali MR, Alaoui AH. Rainfall-Runoff calibration for semi-arid ungauged basins based on the cumulative observed hyetograph and SCS Storm model: Application to the Boukhalef watershed (Tangier, North Western Morocco). J Mater Environ Sci. 2017; 8: 3795-3808.

38. Bo XI, Qing-Hai WA, Jun FA, Feng-Peng HA, Quan-Hou DA. Application of the SCS-CN model to runoff estimation in a small watershed with high spatial heterogeneity. Pedosphere. 2011; 21: 738-749.
39. Jasrotia AS, Dhiman SD, Aggarwal SP. Rainfall-runoff and soil erosion modeling using remote sensing and GIS technique—a case study of tons watershed. J Indian Soc Remote Sens. 2002; 30: 167-180.
40. Satheeshkumar S, Venkateswaran S, Kannan R. Rainfall–runoff estimation using SCS–CN and GIS approach in the Pappiredipatti watershed of the Vaniyar sub basin, South India. Model Earth Syst Environ. 2017; 3: 24.
41. Ranade R, Garg A, Jain S, Pandey K. Satellite Image Enhancement Toolbox (SIET) – an open-source image enhancement implementation. In: Open-Source Geospatial Tools in Climate Change Research and Natural Resources Management. OSGEO-India; 2015. pp. 8-13.
42. Dixit A, Thakur PK, Aggarwal SP, Jain S. Open-source geospatial tools for hydrological modeling. Proceedings of the Second National Conference 'Open-Source Geospatial Tools in Climate Change Research and Natural Resources Management'; 2015 June 8-10; Roorkee, India.
43. United States Department of Agriculture. Soil Conservation service, national engineering handbook. Hydrology section 4. Chapters 4-10. Washington, DC: United States Department of Agriculture; 1972.
44. Bansode A, Patil KA. Estimation of runoff by using SCS curve number method and arc GIS. Int J Sci Eng Res. 2014; 5: 1283-1287.
45. Nalbantis I, Lymperopoulos S. Assessment of flood frequency after forest fires in small ungauged basins based on uncertain measurements. Hydrol Sci J. 2012; 57: 52-72.
46. Leopardi M, Scorzini AR. Effects of wildfires on peak discharges in watersheds. iForest. 2015; 8: 302.
47. Haroon MA, Zhang J, Yao F. Drought monitoring and performance evaluation of MODIS-based drought severity index (DSI) over Pakistan. Nat Hazards. 2016; 84: 1349-1366.
48. Sissay L. Biodiversity potentials and threats to the southern Rift Valley lakes of Ethiopia. In: Wetlands of Ethiopia. IUCN; 2003. pp. 18-24.
49. Pascual-Ferrer J, Shimelis S, Fantaye D, Pérez Foguet A. Research on WASH sector, environment and water resources in the Central Rift Valley of Ethiopia. Proceedings of the IV Congrés Universitat i Cooperació al desenvolupament: Resums de posters i communicacions; 2008 November 12-14; Bellaterra, España. Barcelona: Universitat Autònoma de Barcelona.
50. Friedl M, Sulla-Menashe D. MCD12C1 MODIS/Terra+ Aqua land cover type yearly L3 global 0.05 Deg CMG V006. NASA EOSDIS Land Processes Distributed Active Archive Center; 2015. doi: 10.5067/MODIS/MCD12Q1.006.
51. Hengl T. Soil texture classes (USDA system) for 6 soil depths (0, 10, 30, 60, 100 and 200 cm) at 250 m [Internet]. Genève, Switzerland: Zenodo; 2018. Available from: https://zenodo.org/record/2525817.
52. Funk C, Peterson P, Landsfeld M, Pedreros D, Verdin J, Shukla S, et al. The climate hazards infrared precipitation with stations—a new environmental record for monitoring extremes. Sci Data. 2015; 2: 150066.
53. Ishtiyaq Ahmad IA, Vivek Verma VV, Verma MK. Application of curve number method for estimation of runoff potential in GIS environment. Proceedings of the 2nd International

Conference on Geological and Civil Engineering; 2015 January 10-11; Dubai, UAE. Singapore: IACSIT Press.
54. Hameed HM. Estimating the effect of urban growth on annual runoff volume using GIS in the Erbil sub-basin of the Kurdistan region of Iraq. Hydrology. 2017; 4: 12.
55. Kudoli AB, Oak RA. Runoff estimation by using GIS based technique and its comparison with different methods—a case study on Sangli Micro Watershed. Int J Emerg Res Manag Technol. 2015; 4: 131-137.
56. Sutradhar H. Surface runoff estimation using SCS-CN method in Siddheswari River basin, Eastern India. J Geogr Environ Earth Sci Int. 2018; 17: 1-9.
57. Fuka DR, Walter MT, MacAlister C, Degaetano AT, Steenhuis TS, Easton ZM. Using the Climate Forecast System Reanalysis as weather input data for watershed models. Hydrol Process. 2014; 28: 5613-5623.
58. Schneider DP, Deser C, Fasullo J, Trenberth KE. Climate data guide spurs discovery and understanding. Eos Trans Am Geophys Union. 2013; 94: 121-122.
59. Alsafadi K, Bi S, Bashir B, Hagras A, Alatrach B, Harsanyi E, et al. Land suitability evaluation for citrus cultivation (Citrus ssp.) in the southwestern Egyptian delta: A GIS technique-based geospatial MCE-AHP framework. Arab J Geosci. 2022; 15: 307.
60. Adiat KA, Nawawi MN, Abdullah K. Assessing the accuracy of GIS-based elementary multi criteria decision analysis as a spatial prediction tool–a case of predicting potential zones of sustainable groundwater resources. J Hydrol. 2012; 440: 75-89.
61. Yeh HF, Lin HI, Lee ST, Chang MH, Hsu KC, Lee CH. GIS and SBF for estimating groundwater recharge of a mountainous basin in the Wu River watershed, Taiwan. J Earth Syst Sci. 2014; 123: 503-516.
62. Kumar T, Gautam AK, Kumar T. Appraising the accuracy of GIS-based multi-criteria decision making technique for delineation of groundwater potential zones. Water Resour Manag. 2014; 28: 4449-4466.
63. Rahmati O, Nazari Samani A, Mahdavi M, Pourghasemi HR, Zeinivand H. Groundwater potential mapping at Kurdistan region of Iran using analytic hierarchy process and GIS. Arab J Geosci. 2015; 8: 7059-7071.
64. Arya S, Subramani T, Vennila G, Roy PD. Groundwater vulnerability to pollution in the semi-arid Vattamalaikarai River Basin of south India thorough DRASTIC index evaluation. Geochemistry. 2020; 80: 125635.
65. Boettinger JL, Ramsey RD, Bodily JM, Cole NJ, Kienast-Brown S, Nield SJ, et al. Landsat spectral data for digital soil mapping. In: Digital soil mapping with limited data. Dordrecht, Netherlands: Springer; 2008. pp. 193-202.
66. Barsi JA, Lee K, Kvaran G, Markham BL, Pedelty JA. The spectral response of the Landsat-8 operational land imager. Remote Sens. 2014; 6: 10232-10251.
67. Demir V, Keskin AÜ. Obtaining the Manning roughness with terrestrial-remote sensing technique and flood modeling using FLO-2D: A case study Samsun from Turkey. Geofizika. 2020; 37: 131-156.
68. Ayhan E, Atay G, Erden O. The effect of geometric correction on classification results in high resolutionsatellite images. Proceedings of the Turkey's National Photogrammetry and Remote Sensing Technical Symposium; 2007; İstanbul, Türkiye. pp. 1-5.

69. Adham MI, Shirazi SM, Othman F, Rahman S, Yusop Z, Ismail Z. Runoff potentiality of a watershed through SCS and functional data analysis technique. Sci World J. 2014; 2014: 379763.
70. Mishra SK, Tyagi JV, Singh VP, Singh R. SCS-CN-based modeling of sediment yield. J Hydrol. 2006; 324: 301-322.
71. United States Department of Agriculture. Urban hydrology for small Watersheds. Washington, DC: United States Department of Agriculture; 1986; 210-VI-TR-55.
72. Vinithra R, Yeshodha L. Rainfall–runoff modelling using SCS–CN method: A case study of Krishnagiri District, Tamilnadu. Int J Sci Res. 2016; 5: 2080-2084.
73. Jeon JH, Lim KJ, Engel BA. Regional calibration of SCS-CN L-THIA model: Application for ungauged basins. Water. 2014; 6: 1339-1359.
74. Chow VT, Maidment DK, Mays LW. Applied hydrology. New York, NY: McGraw-Hill Book Company; 1988.
75. Al-Ghobari H, Dewidar A, Alataway A. Estimation of surface water runoff for a semi-arid area using RS and GIS-based SCS-CN method. Water. 2020; 12: 1924.
76. Matomela N, Tianxin L, Morahanye L, Bishoge OK, Ikhumhen HO. Rainfall-runoff estimation of Bojiang lake watershed using SCS-CN model coupled with GIS for watershed management. J Appl Adv Res. 2019; 4: 16-24.
77. Rallison RE. Origin and evolution of the SCS runoff equation. In: Proceedings of ASCE irrigation and drainage division symposium on watershed management. New Delhi: ASCE; 1980. pp. 912-924.
78. Méllo Júnior AV, Olivos LM, Billerbeck C, Marcellini SS, Vichete WD, Pasetti DM, et al. Rainfall runoff balance enhanced model applied to tropical hydrology. Water. 2022; 14: 1958.
79. Patil JP, Sarangi A, Singh AK, Ahmad T. Evaluation of modified CN methods for watershed runoff estimation using a GIS-based interface. Biosyst Eng. 2008; 100: 137-146.
80. Mishra SK, Singh VP. Soil conservation service curve number (SCS-CN) methodology. In: Water Science and Technology Library. Dordrecht: Kluwer Academic Publishers; 2003.
81. Woodward DE, Hawkins RH, Jiang R, Hjelmfelt, Jr AT, Van Mullem JA, et al. Runoff curve number method: Examination of the initial abstraction ratio. Proceedings of the 2003 World Water and Environmental Resources Congress; 2023 June 23-26; Philadelphia, PA, USA. Reston, VA: ASCE.
82. Amutha R, Porchelvan P. Estimation of surface runoff in Malattar sub-watershed using SCS-CN method. J Indian Soc Remote Sens. 2009; 37: 291-304.
83. Kumari M, Kalita P, Mishra VN, Choudhary A, Abdo HG. Rainfall-runoff modelling using GIS based SCS-CN Method in Umiam Catchment Region, Meghalaya, India. Phys Chem Earth Parts A/B/C. 2024; 135: 103634.
84. Patel J, Singh NP, Prakash I, Mehmood K. Surface runoff estimation using SCS-CN method-a case study on Bhadar Watershed, Gujarat, India. Imp J Interdiscip Res. 2017; 3: 1213-1218.
85. Reddy DM, Lalitha R. Rainfall-Runoff Analysis using Runoff Coefficient and SCS-CN Methods under GIS Approach. Int J Environ Clim Change. 2021; 11: 148-157.
86. Nandhakumar S, Arsheya S, Sri VK. Estimation of Rainfall Runoff using SCS-CN and GIS Approach in Puzhal Watershed. Int J Civil Eng Technol. 2019; 10: 1978-1998.
87. Saha A, Pal SC, Santosh M, Janizadeh S, Chowdhuri I, Norouzi A, et al. Modelling multi-hazard threats to cultural heritage sites and environmental sustainability: The present and future scenarios. J Clean Prod. 2021; 320: 128713.

88. Pal SC, Chakrabortty R, Roy P, Chowdhuri I, Das B, Saha A, et al. Changing climate and land use of 21st century influences soil erosion in India. Gondwana Res. 2021; 94: 164-185.
89. Umukiza E, Raude JM, Wandera SM, Petroselli A, Gathenya JM. Impacts of land use and land cover changes on Peakdischarge and flow volume in Kakia and Esamburmbur sub-catchments of Narok town, Kenya. Hydrology. 2021; 8: 82.
90. United States Department of Agriculture Soil Conservation Service. Soil survey of Travis County. Washington DC, USA: United States Department of Agriculture Soil Conservation Service; 1974.
91. Liu X, Li J. Application of SCS model in estimation of runoff from small watershed in Loess Plateau of China. Chin Geogr Sci. 2008; 18: 235-241.
92. Feldman AD. Hydrologic modeling system HEC-HMS: Technical reference manual. Davis, CA: US Army Corps of Engineers, Hydrologic Engineering Center; 2000.
93. Zhan X, Huang ML. ArcCN-Runoff: An ArcGIS tool for generating curve number and runoff maps. Environ Model Softw. 2004; 19: 875-879.
94. Shrestha MN. Spatially distributed hydrological modelling considering land-use changes using remote sensing and GIS [Internet]. Geospatial World; 2003. Available from: https://citeseerx.ist.psu.edu/document?repid=rep1&type=pdf&doi=966ebfedaf68053580a6ae38b7ac63967ac28322.
95. Kumar Mishra S, Gajbhiye S, Pandey A. Estimation of design runoff curve numbers for Narmada watersheds (India). J Appl Water Eng Res. 2013; 1: 69-79.
96. Sindhu D, Shivakumar BL, Ravikumar AS. Estimation of surface runoff in Nallur Amaniker watershed using SCS-CN method. Int J Res Eng Technol. 2013; 4: 404-409.
97. Das B, Pal SC, Malik S, Chakrabortty R. Modeling groundwater potential zones of Puruliya district, West Bengal, India using remote sensing and GIS techniques. Geol Ecol Landsc. 2019; 3: 223-237.
98. Zhang Y, Vaze J, Chiew FH, Teng J, Li M. Predicting hydrological signatures in ungauged catchments using spatial interpolation, index model, and rainfall–runoff modelling. J Hydrol. 2014; 517: 936-948.
99. Zhang G, Zhang X, Hu X. Runoff and soil erosion as affected by plastic mulch patterns in vegetable field at Dianchi lake's catchment, China. Agric Water Manag. 2013; 122: 20-27.
100. Topno A, Singh AK, Vaishya RC. SCS CN runoff estimation for Vindhyachal region using remote sensing and GIS. Int J Adv Remote Sens GIS. 2015; 4: 1214-1223.
101. Kimura R, Fan J, Zhang X, Takayama N, Kamichika M, Matsuoka N. Evapotranspiration over the grassland field in the Liudaogou Basin of the Loess Plateau, China. Acta Oecol. 2006; 29: 45-53.
102. Vaze J, Post DA, Chiew FH, Perraud JM, Viney NR, Teng J. Climate non-stationarity–validity of calibrated rainfall–runoff models for use in climate change studies. J Hydrol. 2010; 394: 447-457.
103. Qiu Y, Fu B, Wang J, Chen L. Spatial variability of soil moisture content and its relation to environmental indices in a semi-arid gully catchment of the Loess Plateau, China. J Arid Environ. 2001; 49: 723-750.
104. Marhaento H, Booij MJ, Hoekstra AY. Hydrological response to future land-use change and climate change in a tropical catchment. Hydrol Sci J. 2018; 63: 1368-1385.
105. Gyamfi C, Ndambuki JM, Salim RW. Hydrological responses to land use/cover changes in the Olifants Basin, South Africa. Water. 2016; 8: 588.

106. Arulbalaji P, Maya K. Effects of land use dynamics on hydrological response of watershed: A case study of Chittar watershed, Vamanapuram River Basin, Thiruvananthapuram District, Kerala, India. Water Conserv Sci Eng. 2019; 4: 33-41.
107. Chen Z, Liu X, Zhu B. Runoff estimation in hillslope cropland of purple soil based on SCS-CN model. Trans Chin Soc Agric Eng. 2014; 30: 72-81.
108. Khan A, Govil H, Taloor AK, Kumar G. Identification of artificial groundwater recharge sites in parts of Yamuna River basin India based on Remote Sensing and Geographical Information System. Groundw Sustain Dev. 2020; 11: 100415.
109. Kannaujiya S, Gautam PK, Chauhan P, Roy PN, Pal SK, Taloor AK. Contribution of seasonal hydrological loading in the variation of seismicity and geodetic deformation in Garhwal region of Northwest Himalaya. Quat Int. 2021; 575: 62-71.
110. Taloor AK, Kothyari GC, Manhas DS, Bisht H, Mehta P, Sharma M, et al. Spatio-temporal changes in the Machoi glacier Zanskar Himalaya India using geospatial technology. Quat Sci Adv. 2021; 4: 100031.
111. Peng DZ. Application of improved SCS model in runoff simulation of river basin. J Water Resour Water Eng. 2006; 17: 20-24.
112. Evett SR, Dutt GR. Length and slope effects on runoff from sodium dispersed, compacted earth microcatchments. Soil Sci Soc Am J. 1985; 49: 734-738.
113. Potter NJ, Chiew FH. An investigation into changes in climate characteristics causing the recent very low runoff in the southern Murray-Darling Basin using rainfall-runoff models. Water Resour Res. 2011; 47: W00G10.
114. Chiew FH, Zheng H, Potter NJ. Rainfall-runoff modelling considerations to predict streamflow characteristics in ungauged catchments and under climate change. Water. 2018; 10: 1319.
115. Zende AM, Nagarajan R, Atal KR. Analysis of surface runoff from Yerala River Basin using SCS-CN and GIS. Int J Geomat Geosci. 2014; 4: 508-516.
116. Rizeei HM, Pradhan B, Saharkhiz MA. Surface runoff prediction regarding LULC and climate dynamics using coupled LTM, optimized ARIMA, and GIS-based SCS-CN models in tropical region. Arab J Geosci. 2018; 11: 53.
117. Mohtar WH, Maulud KN, Muhammad NS, Sharil S, Yaseen ZM. Spatial and temporal risk quotient-based river assessment for water resources management. Environ Pollut. 2019; 248: 133-144.
118. Soulis KX. Soil conservation service curve number (SCS-CN) Method: Current applications, remaining challenges, and future perspectives. Water. 2021; 13: 192.
119. Shyam GM, Taloor AK, Singh SK, Kanga S. Sustainable water management using rainfall-runoff modeling: A geospatial approach. Groundw Sustain Dev. 2021; 15: 100676.
120. Adnan RM, Petroselli A, Heddam S, Santos CA, Kisi O. Short term rainfall-runoff modelling using several machine learning methods and a conceptual event-based model. Stoch Environ Res Risk Assess. 2021; 35: 597-616.
121. Mittal N, Bhave AG, Mishra A, Singh R. Impact of human intervention and climate change on natural flow regime. Water Resour Manag. 2016; 30: 685-699.
122. Falkenmark M. Water and sustainability: A reappraisal. Environment. 2008; 50: 4-17.